


TECHNICAL UNIVERSITY MUNICH

DEPARTMENT OF MATHEMATICS

CHAIR OF MATHEMATICAL MODELLING

Mathematical Models for Morphological Conversion of *Pseudomonas Aeruginosa* in Response to Beta-Lactam Antibiotics

MASTER'S THESIS

Author:
Rebekka Müller
rebekka.mueller@tum.de

Supervisor/Advisor:
Prof. Dr. Christina Kuttler
kuttler@ma.tum.de

Submission date: 07/08/2017

Declaration of Authorship

I, Rebekka Müller, hereby declare that this thesis

"Mathematical Models for Morphological Conversion of Pseudomonas Aeruginosa in Response to Beta-Lactam Antibiotics"

is my own work and that no other sources have been used except those clearly indicated and referenced.

Neufahrn, 07/08/2017

Rebekka Müller

Abstract

The pathogen *Pseudomonas aeruginosa* is commonly treated with beta-lactam antibiotics. However, the bacterium's antibiotic resistance is a severe problem in which a morphological conversion plays an important role. The cells have the ability to rapidly convert from rods into spherically shaped cells, which are highly tolerant of antibiotic stress. In this thesis we set up, analyse, and compare different mathematical models for these biological findings. The first model does not include any specific biological assumptions about the conversion process. The second approach is based on the concept of quorum sensing and presumes that the cell-cell communication regulates the bacteria's response to antibiotics. To complete the thesis we present several modifications of the basic models and compare them.

Contents

List of Figures

List of Tables

List of Abbreviations

ACP	**A**cyl **C**arrier **P**rotein
AHL	**A**cyl **H**omoserine **L**actone
AMP	**A**nti **M**icrobial **P**eptide
MIC	**M**inimum **I**nhibitory **C**oncentration
MLE	**M**aximum **L**ikelihood **E**stimate
ODE	**O**rdinary **D**ifferential **E**quation
QS	**Q**uorum **S**ensing
SAM	**S**-**A**denosyl **M**ethionine

Introduction

In this thesis we set up, analyse, and compare different mathematical models for the morphological conversion of the bacterium *Pseudomonas aeruginosa* in response to beta-lactam antibiotics. The underlying biological findings were published by an Australian research group in the article "*Rapid Conversion of Pseudomonas aeruginosa to a Spherical Cell Morphotype Facilitates Tolerance to Carbapenems and Penicillins but Increases Susceptibility to Antimicrobial Peptides*" by Monahan et al. [25]. Before going into a detailed description of their results, we first introduce relevant biological terms and concepts, and start with presenting the bacterium of interest - *Pseudomonas aeruginosa*.

1.1 Biological Background

1.1.1 Pseudomonas Aeruginosa

P. aeruginosa is a prevalent, rod-shaped bacterium arising in moist environments like soil, water, or skin flora, but it can also be found in medical equipment like catheters or prostheses. It belongs to the group of Gram-negative bacteria, which have characteristic cell envelopes that consist of an inner cytoplasmic cell membrane, a cell wall, and a bacterial outer membrane. This human pathogen is a leading cause of hospital-acquired infections [25] with a high mortality rate [15, 17]. Typical infections show up during already existing diseases such as cystic fibrosis and are provoked in the airway, the urinary tract, burns, and wounds. As many other bacteria, *P. aeruginosa* form a biofilm, which means that the cells accumulate and are embedded in a kind of slime. This biofilm formation serves as protection against adverse conditions. Yet colonising in the human body also represents a strategy to overwhelm the immune system.
Therapies are mainly based on beta-lactams, which will be introduced in more detail shortly. However, being intrinsically multidrug resistant it is a severe problem to treat the bacterium efficiently. The resistance is acquired from the bacterium's metabolism, which for example allows for the just mentioned biofilm formation. But it also comes from the property to loose or alter its outer cell membrane inhibiting or at least limiting the entry of antimicrobials [31]. There are different suggestions for more efficient treatments. As proposed in [25], one is to combine beta-lactam with antimicrobial peptides. Another approach arises from the finding that environmental stress influences cell-cell communication, the so-called quorum sensing mechanism, which will be discussed later. This could play an important role for bacterial resistance and thus makes it a potential target.

1.1.2 Beta-Lactam Antibiotics

Beta-lactam antibiotics are the world's most widely used antibiotic agents acting against numerous and diverse disease-causing bacteria [25]. The name is derived

from their common beta-lactam ring in the molecular structure. The class of beta-lactam antibiotics consists of different groups, which are subdivided further. Penicillins represent one famous group with carbenicillin as an exemplary agent. Another group are carbapenems, which have among other representatives imipenem and meropenem [31]. Their bactericidal activity works by inhibiting cell wall biosynthesis of bacteria [12], which occurs during cell division. Since this metabolism does not happen in humans, beta-lactam antibiotics are normally well tolerated, however allergies may appear as reaction [23].
Resistance of bacteria against beta-lactam antibiotics is an increasing problem. Bacteria developed different mechanisms to resist adverse attacks. Besides the previously mentioned membrane alteration, another strategy of them is to synthesise beta-lactamase, an enzyme, which attacks the beta-lactam ring of the antibiotic, see for instance [12].

1.1.3 Antimicrobial Peptides

Antimicrobial peptides (AMPs) are organic compounds of amino acids. They can mainly be found in organs and tissues exposed to airborne pathogens [3] and show important and broad antimicrobial properties against different targets including bacteria, viruses, fungi, and parasites [18, 3]. They can target the membrane or interact with intracellular targets of the microorganisms, inhibit synthesis of proteins, DNA, and RNA [3], and kill in seconds after the first contact. Hence, AMPs operate as a host's first-line defence system, whose activity is increased in case of injury to stop infections before any symptoms occur. In addition to this first-line defence, AMPs also interact with the host's repair and adaptive immune responses [18]. In combination with antibiotics they can improve the microbicidal effects [3].
The increasing problems regarding resistance against common antibiotics emphasise the importance of AMPs as alternative control agents [3]. Several thousand AMPs have been discovered or synthesised. Artificial peptides are produced for different reasons; one can change targets of AMPs and their own stability can be improved [3]. However, despite the useful properties of AMPs there are some drawbacks: it is expensive to produce AMPs and the peptides are sensitive to harsh environmental conditions as for example extreme pH values. Furthermore, possible toxic effects on humans have to be clarified and some bacteria are already known to be resistant to various AMPs [3].

With this introduction of the most important terms we can now address the biological findings which represent the basis of the mathematical part in this thesis.

1.2 Biological Findings

The researchers in [25] examined and discussed the question why *P. aeruginosa* are tolerant to treatments with high concentrations of beta-lactam. It was already known before that these antibiotics inhibit the bacteria's growth, albeit their bactericidal effect is unusually little. The main statement of the paper is that "*P. aeruginosa* undergoes a rapid *en masse* transition from normal rod-shaped cells to viable cell wall-defective spherical cells when treated with beta-lactams" [25]. Remarkably, the bacterial population is able to reconvert from the spherical shape into the initial rod form, and all transformations take place rather rapidly. These findings give

an additional insight into the bacteria's survival strategy under antibiotic stress. Furthermore, the biologists came up with an approach to make use of the fragility and sensitivity of the bacteria in their spherical shape after treatment with carbapenem. Spherical cells are efficiently killed when carbapenem treatment is combined with AMPs.
To recapitulate, carbapenem treatment is used to induce a transition into a spherical cell shape. This type of cells can be in turn targeted with AMPs, which themselves are inactive against the normal bacillary cells of *P. aeruginosa*. Hence, in combination the two components may present an efficient treatment.

1.2.1 Experiments

For a detailed description and more precise data of the experiments we refer to [25]. Shortly summarised, the biologists used different strains of *P. aeruginosa* and grew them on various standard laboratory growth media but also in environments mimicking physiologically relevant conditions during infections occurring for example in a cystic fibrosis lung. Beta-lactam antibiotics meropenem, imipenem, and carbenicillin were added at $5 \times$ MIC, where MIC stands for the "minimum inhibitory concentration", the lowest concentration of a chemical or an antimicrobial drug that inhibits visible growth of a microorganism. The MIC values for the mainly used strain PA14 are given in table 1.1.

Beta-lactam	**MIC value**
Meropenem	$1\,\mu g\,mL^{-1}$
Imipenem	$2\,\mu g\,mL^{-1}$
Carbenicillin	$128\,\mu g\,mL^{-1}$

Table 1.1: MIC values for strain PA14. Adapted from [25].

For the reversion of the morphological transformation, samples were resuspended in antibiotic-free media. In order to verify their hypothesis that beta-lactams together with AMPs may present an efficient treatment, meropenem was used together with different concentrations of the AMPs LL-37 and nisin.
The exact setup of the used phase-contrast, fluorescence, and transmission electron microscopy can be found in [25].

1.2.2 Observations

Conversion

Treating a culture of *P. aeruginosa* PA14 with the above reported dose ($5 \times$ MIC) of meropenem, the whole population converts quickly from normal rod-shaped into spherical cells (figure 1.1a). The transformation starts with a small protrusion of the membrane on the cell surface. There the cell bulges out forming a sphere, which is enclosed in its own membrane, and leads to lysis of the rod (figure 1.1b). However, the spheres become highly fragile and lack a functional cell wall: the original double-membrane is destroyed since the outer membrane is disrupted and the inner one becomes exposed on the surface [25]. This is an example of how the cell wall-targeting beta-lactam antibiotic provokes a change of the cell wall and membrane.
This rapid process is summarised in figure 1.2. After one hour more than half of the total population (65%) started to transform its shape. After another three hours 67%

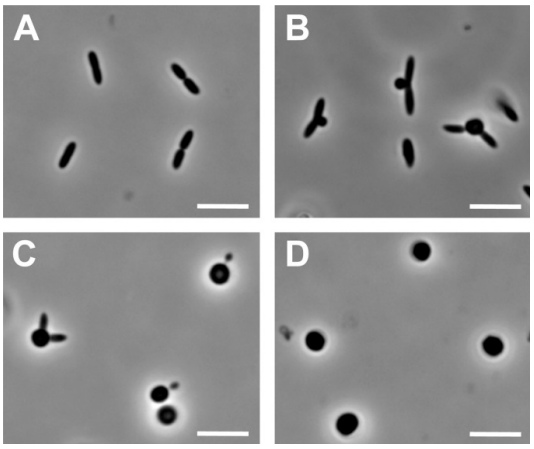

(a) Phase-contrast images were taken before the treatment with meropenem, after 1h, 4h, and 24h (A-D). Scale bars, 5 µm.

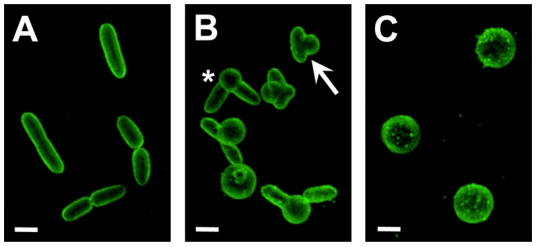

(b) Conversion depicted by superresolution 3D-SIM microscopy. Images were taken 0h, 2h, and 24h (A-C) after beta-lactam addition. Scale bars, 1 µm.

Figure 1.1: Conversion of *P. aeruginosa* to spherical cells in response to presence of meropenem. Adapted from [25].

of the cells were in spherical shape, and after one day the entire population changed its appearance.

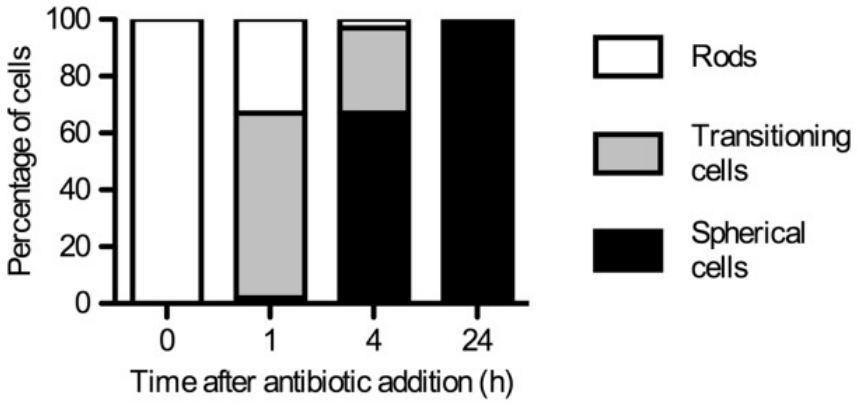

Figure 1.2: Proportion of rods, transitioning, and spherical cells in the meropenem-treated population over 24 h. Adapted from [25].

By fluorescence microscopy of LIVE/DEAD stained cells the viability of spherical cells was determined. It was found that 84% of the cells were viable and only 16% did not tolerate the applied amount of antibiotics. Moreover, dead cells were also detectable without any staining due to their "ghostlike appearance" [25] as can be seen in figure 1.3. Additionally, the researchers found that the number of viable cells could be increased from 84% to 97% by providing the growth medium with 0.5 M sucrose; here M is an abbreviation for the unit mol/litre. The addition of sucrose is not essential for the observations themselves but it is useful to reduce the number of lysed cells by acting as an osmoprotectant: antibiotics damage the bacterium's cell wall which leads to osmotic stress and finally lysis of cells. Sucrose extenuates this osmotic stress.

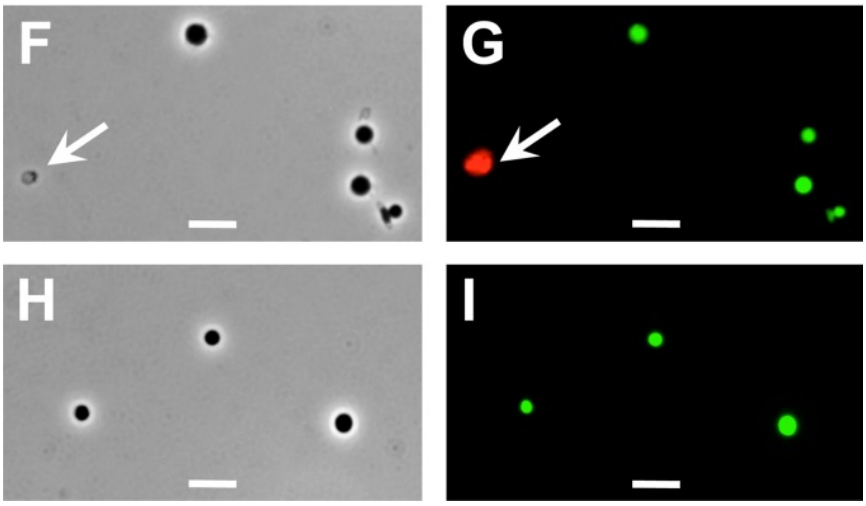

Figure 1.3: Phase contrast microscopy (F and H) and fluorescence microscopy (G and I) visualise meropenem-treated samples after 24h under LIVE/DEAD staining. (F and G) show cells grown in a standard growth medium, (H and I) cells grown in the same medium supplemented with 0.5 M sucrose. Arrows show lysed cells. Scale bars, $5\,\mu\mathrm{m}$. Adapted from [25].

Reversion

Interestingly, the bacteria are able to revert the whole transformation as rapidly as before when antibiotics are removed. When the spherical cells are put into a fresh medium without any drugs, the cellular population first changes to an ellipsoid morphology, before the shape is further transformed back into the normal rod form, which is shown in figure 1.4a. Some cells changed into ellipsoid shape even after just half an hour.
Figure 1.4b shows that more than 90% of the population completed its reversion after 6 hours. Back in the normal bacillary cell form they can develop and reproduce as usual [25] indicating that the whole process serves as survival strategy: the cells are temporarily robust against adverse conditions, and after rapid reversion the population is able to grow again.

The researchers did not only use meropenem, but also carbenicillin and imipenem, for which the observations were similar. In the case of carbenicillin some cells became filamentous and tended to lyse [25]. By that, the bacterium's response to beta-lactams is shown for agents of two different classes. Since the observations do not depend on a specific strain of the bacterium or on its genetic background, the protection strategy is assumed to be an intrinsic property of *P. aeruginosa* [25].

Treatment with a Combination of Beta-Lactams and AMPs

The spherically shaped cells have a deficient cell wall after being treated with beta-lactam. Therefrom the researchers came up with the hypothesis that this weakness could be exploited by AMPs, which kill the spherical cells by forming pores in their membranes. Actually they could verify their hypothesis combining meropenem, which itself induces conversion to viable spherical cells, with different concentrations of the AMPs LL-37 and nisin. AMPs alone had very little effect on the normal bacillary cells, but they noticeable reduced the spherical cells' viability [25]. These

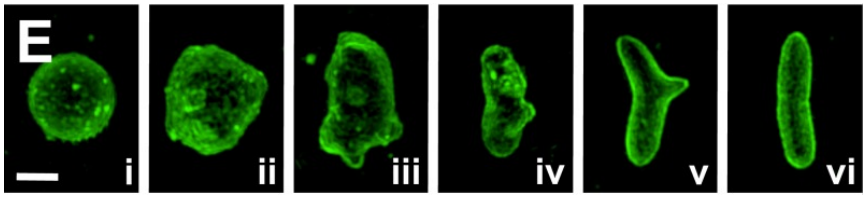

(a) Transition from spheres back to normal rods. Scale bars, 1 µm.

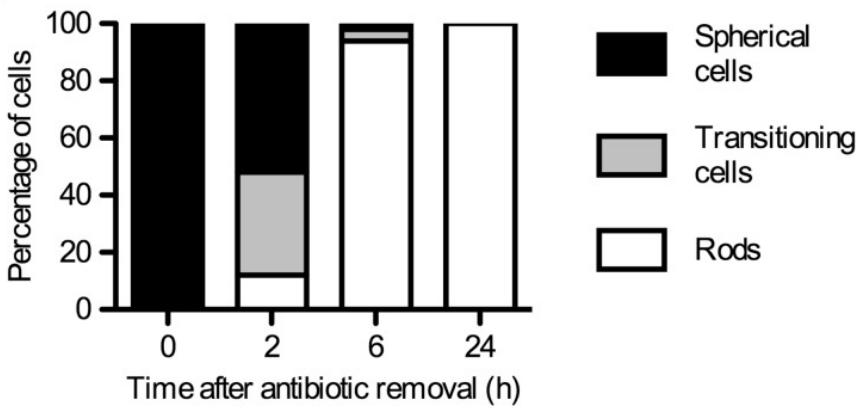

(b) Proportion of rods, transitioning, and spherical cells in the population over 24h.

Figure 1.4: Reversion of *P. aeruginosa* from spherical cells back to rods after removal of meropenem. Adapted from [25].

findings show that the drug combination of beta-lactam and AMPs are indeed effective and could be a novel treatment against *P. aeruginosa*.

One of the remaining open questions is the underlying mechanism that is responsible for the conversion of the cells. A potential explanation could be the so-called quorum sensing, a cell-cell communication. Since we will use this approach later in the mathematical models, the concept will be introduced before starting with the mathematical part of this thesis.

1.3 Quorum Sensing

Quorum sensing (QS) is a well-known concept of cell-cell communication within and between different species of bacteria. Individual bacteria produce and release so-called autoinducers, which are chemical signal molecules, whose concentration depends on changes in the cell density. These diffusible molecules can be detected by surrounding organisms [36]. Above a certain threshold the concentration of these signal molecules leads to an alteration in gene expression. This regulation affects plenty of physiological activities such as symbiosis, virulence, biofilm formation, and motility [24], and protects the cells against environmental stresses [14]. This mechanism enables the bacteria to "indirectly monitor changes in their own population density" [7] and to act as a whole community in order to lead the collective behaviour in the best way to survive and be robust against adverse conditions.
The QS network of *P. aeruginosa* is organised in a multi-layered hierarchy consisting of at least four interconnected signalling mechanisms [22]. As for most Gram-negative bacteria the signal molecules are acyl homoserine lactones (AHLs). The *las* system was one of the first studied QS systems. It involves two components:

the LasR transcriptional regulator and the LasI synthase protein. This protein is necessary for the production of the AHL signal molecule N-(3-oxododecanoyl)-L-homoserine lactone (3O-C_{12}-HSL). LasR needs to bind to this complex to become an active transcriptional regulator and to form multimers. These then bind to DNA and regulate gene transcription [36]. A visualisation of this system is depicted in figure 1.5. Another QS system of *P. aeruginosa* regulates several genes with a complex consisting of RhlR proteins and C_4-HSL (N-butyryl-L-homoserine lactone), which is produced by RhlI synthase [36, 24].

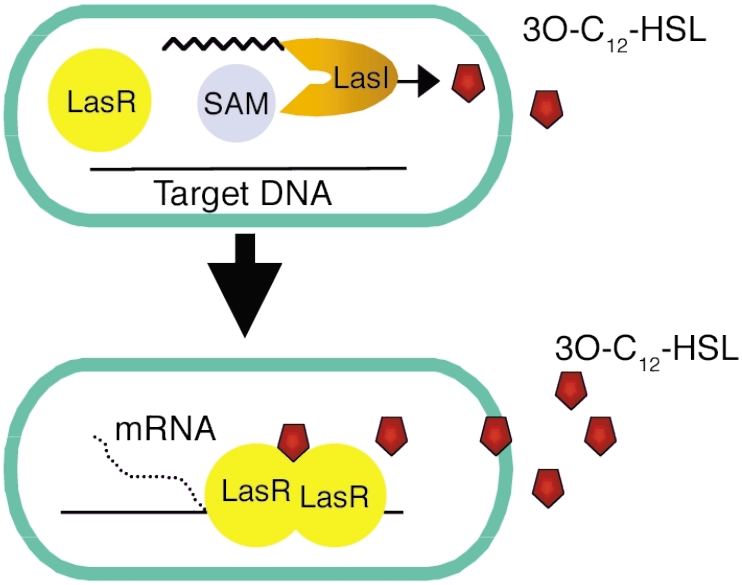

Figure 1.5: The QS system *las* of *P. aeruginosa*. LasI synthase uses S-adenosyl methionine (SAM) and acyl-acyl carrier protein (acyl-ACP) to form the AHL 3O-C_{12}-HSL. With increasing concentration the AHL molecule binds to the LasR regulator leading to dimerisation of LasR molecules. These dimers bind to the DNA and hereby activate the transcription of several genes. Adapted from [36].

Meanwhile other QS systems of *P. aeruginosa* were detected and their interaction is studied in more detail. The known QS signalling mechanisms besides *las* and *rhl* are *pqs* and *iqs*. However, for deeper insight into the topic we refer to [22] .
It is known that "functional QS systems significantly affect the severity" [36] of *P. aeruginosa* infections. An approach for new treatments and strategies against the resistance of bacteria is to use the QS system as target. Due to the wide interaction of the different QS systems, it is not sufficient to attack only a single system but the whole network has to be understood better in order to know which parts of it have to be switched off.

We now have the necessary knowledge about the biological observations and concepts and can start to formulate mathematical models for the findings.

The Naive Model

In this chapter we are going to use the results of [25] and set up a first model for the dynamics of the transition from rod to spherical shape of *P. aeruginosa* under treatment with beta-lactam antibiotics. We call it the Naive Model since it does not include any specific biological assumptions about the transition process. After introducing the model, we will first fit its parameters to the observed data, before analysing it with respect to fixed points and their stability, maintenance of positivity, and boundedness of the system. At the end of this chapter a modification of the Naive Model and the dynamics of the reverse transformation of *P. aeruginosa* back to rod shape will be presented shortly. Some ideas for the models in the following chapters are taken from the publication "*Quorum Sensing Interaction and the Effect of Antibiotic on the Dynamics of Two Strains of the Same Bacterial Species*" by Campos et al. [7].

2.1 Model Variables, Assumptions, and Parameters

Model Variables

The authors in [25] distinguish three different types of bacteria depending on their shape. Hence it is natural to include this classification in our model by using three different types A, T, and B for bacteria of natural rod shape, transitioning shape, and spherical shape respectively. For mathematical notation we introduce the variables $A(t)$, $T(t)$, and $B(t)$ which denote the population densities of bacteria of type A, T, and B at time t. Furthermore, the variable $C(t)$ is defined as the concentration of beta-lactam antibiotics to which the bacteria are exposed at time t.
Table 2.1 gives an overview of these variables together with units that are commonly used in biological models, see for example [7].

Variable	Meaning	Unit
$A(t)$	Population density of *P. aeruginosa* of type A (natural rod shape)	$\text{cells}\,\text{mL}^{-1}$
$T(t)$	Population density of *P. aeruginosa* of type T (transitioning shape)	$\text{cells}\,\text{mL}^{-1}$
$B(t)$	Population density of *P. aeruginosa* of type B (spherical shape)	$\text{cells}\,\text{mL}^{-1}$
$C(t)$	Concentration of beta-lactam	$\mu\text{g}\,\text{mL}^{-1}$

Table 2.1: Variables of the Naive Model, cf. [7].

Assumptions and Model Parameters

The concentration of beta-lactam $C(t)$ in the system can be controlled exogenously by a constant supply rate θ. Moreover the concentration is decreased with degradation rate λ. We assume that the population density of bacteria of type A underlies a logistic growth $r_a A(t)\,(1 - A(t)/K_a)$ with growth rate r_a and carrying capacity K_a. This growth model is often used in similar contexts, cf. for example [7]. Ordinary death is already incorporated in the growth term. In contrast, the addition of beta-lactam leads to further deaths, which we highlight by introducing an extra death rate ε_β in our model. The concentration of cells of type A is also decreased by a rapid conversion into type T with probability ω_1. This conversion follows the law of mass action but there is no particular mechanism modelled for the transition. Under the assumption that the dynamics regarding cells of type T are fast, we disregard for simplicity any natural death or death caused by beta-lactam for cells of type T, and only the conversion to cells of type B is incorporated by the mass action coefficient ω_2. According to the descriptions in [25], cells of type B do not seem to reproduce. As it is stated ibid., type B cells are resistant to beta-lactam antibiotics, and therefore in our model only natural death with rate δ_n is assumed. Figure 2.1 depicts the model setting in a flow diagram.

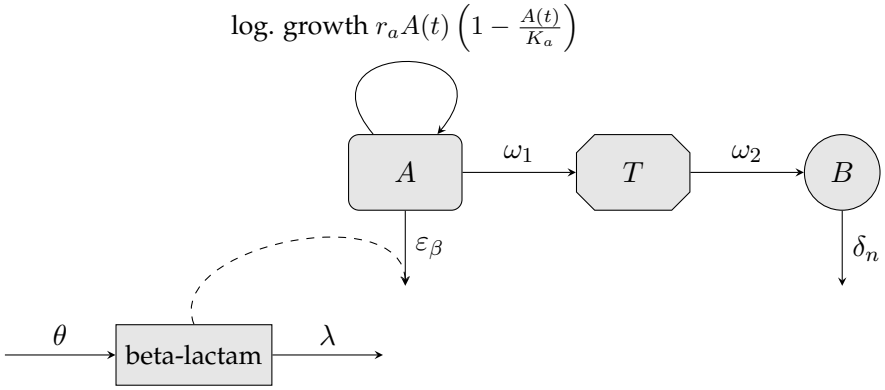

Figure 2.1: Flow diagram of the Naive Model.

Remark 1 Generally for this thesis we assume that all parameters and variables are non-negative and real-valued in order to obtain a biologically meaningful model. $\diamond$

If we suppose that all components in the system are homogeneously mixed, we can neglect any spatial distribution of the bacteria and the above assumptions lead to the following dynamical system of ordinary differential equations (ODEs):

$$\frac{dA}{dt}(t) = \underbrace{r_a A(t)\left(1 - \frac{A(t)}{K_a}\right)}_{\text{log. growth}} - \underbrace{\varepsilon_\beta A(t) C(t)}_{\text{death by beta-lactam}} - \underbrace{\omega_1 A(t)}_{\text{conversion to } T} \tag{2.1}$$

$$\frac{dT}{dt}(t) = \underbrace{\omega_1 A(t)}_{\text{conversion to } T} - \underbrace{\omega_2 T(t)}_{\text{conversion to } B} \tag{2.2}$$

$$\frac{dB}{dt}(t) = \underbrace{\omega_2 T(t)}_{\text{conversion to } B} - \underbrace{\delta_n B(t)}_{\text{natural death}} \tag{2.3}$$

$$\frac{dC}{dt}(t) = \underbrace{\theta}_{\text{supply}} - \underbrace{\lambda C(t)}_{\text{degradation}} \tag{2.4}$$

Together with some initial values $A(t_0)$, $T(t_0)$, $B(t_0)$, and $C(t_0)$ at a starting time t_0 the system of equations (2.1) to (2.4) becomes an initial value problem. The parameters introduced above are summarised in table 2.2 with corresponding units.

Parameter	Meaning	Unit
r_a	Intrinsic growth rate of type A	h^{-1}
K_a	Carrying capacity of type A	$\mathrm{cells}\,\mathrm{mL}^{-1}$
ε_β	Death rate of type A due to beta-lactam	$\mathrm{mL}\,\mathrm{h}^{-1}\,\mu\mathrm{g}^{-1}$
ω_1	Mass action coeff. for change from type A into type T	h^{-1}
ω_2	Mass action coeff. for change from type T into type B	h^{-1}
δ_n	Natural death rate of type B	h^{-1}
θ	Supply rate of beta-lactam	$\mu\mathrm{g}\,\mathrm{mL}^{-1}\,\mathrm{h}^{-1}$
λ	Degradation rate of beta-lactam	h^{-1}

Table 2.2: Parameters of the Naive Model, cf. [7].

Certainly there are further experimental conditions like growth medium, oxygen concentration, and pH value, that influence the dynamics and interactions of the bacteria and beta-lactam. But it is not possible to catch all biological circumstances precisely, and probably it is neither necessary in order to capture and understand the behaviour observed biologically for certain parameter values.

2.2 Parameter Fitting and Evaluation

Overview

To investigate whether the dynamical system (2.1) to (2.4) can exhibit a similar behaviour as the researchers found in [25], we first fit the parameters of the Naive Model to the experimental results. Unfortunately the paper only provides very vague data in form of figure 1.2 and a few values in the description of the results. We use these values and bar charts in figure 1.2 for parameter fitting by extracting the proportions of the three types A, T, and B at the four shown time points. Inaccuracy arises already here from using the naked eye for this extraction. The aim is then to find parameter values, including initial values, of the model given by equations (2.1) to (2.4) such that the calculated theoretical proportions of these three types at the corresponding time points fit the deduced data best. The best fit is obtained by minimising the least squares function of the given and the computed data using a multi-start approach, cf. listing 3. For given parameters we calculate the theoretical proportions of the types by solving the ODE system of equations (2.1) to (2.4) and normalise the resulting concentrations at the four time points, cf. listing 2.

Mathematical Explanations

For estimating parameters which provide us with the best fit of theoretical calculations to measurement data, we start with applying the common maximum likelihood approach. As its name suggests, this method maximises the likelihood of observing the measured data with our model given a vector $\Theta \in \mathbb{R}^k$ of parameters, where k is the total number of parameters.
At first we introduce some notations that are used in the following section. Let the extracted experimental data points be denoted by a matrix $\hat{\mathcal{D}} \in \mathbb{R}^{4\times 3}$, where the observations at the four time points are given by the rows $\hat{d}_i \in \mathbb{R}^3$, $i \in \{1, \ldots, 4\}$.

Analogously, the corresponding theoretical data points are denoted by a matrix $\mathcal{D} = \mathcal{D}(\Theta) \in \mathbb{R}^{4\times 3}$ with corresponding rows $d_i \in \mathbb{R}^3$, $i \in \{1,\dots,4\}$, which as indicated depends on the chosen parameters.
Under the assumption that the observations $\hat{d}_i$, $i \in \{1,\dots,4\}$, are independent, or to be more precise, the underlying random variables that generated those realisations, the joint density function f is given by

$$f(\hat{d}_1,\hat{d}_2,\hat{d}_3,\hat{d}_4|\Theta) = f_1(\hat{d}_1|\Theta)\times f_2(\hat{d}_2|\Theta)\times f_3(\hat{d}_3|\Theta)\times f_4(\hat{d}_4|\Theta) \tag{2.5}$$

with marginal density functions f_i, $i \in \{1,\dots,4\}$. If we further assume that the single observations are identically distributed around the "true" data d_i, $i \in \{1,\dots,4\}$, and in particular follow a three-dimensional normal distribution with covariance matrix $\sigma^2 I_3$ for some $\sigma^2 \geq 0$, we can specify the marginal density functions:

$$\begin{aligned} f_i(\hat{d}_i|\Theta) &= \frac{1}{\sqrt{(2\pi)^3\det(\sigma^2 I_3)}}\exp\left(-\frac{1}{2}(\hat{d}_i - d_i)^T\frac{1}{\sigma^2}I_3(\hat{d}_i - d_i)\right) \\ &= \frac{1}{\sqrt{(2\pi\sigma^2)^3}}\exp\left(-\frac{1}{2\sigma^2}||\hat{d}_i - d_i||_2^2\right). \end{aligned}$$

Remark 2 If the random variables which generate the observations $\hat{d}_i$, with $i \in \{1,\dots,4\}$, are dependent, equation (2.5) does not hold in general. Even under the assumption that they follow a normal distribution, we do not know the joint density function. This problem can only be circumvented to the expense of additional assumptions like a joint normal distribution. Since we obtain satisfying results when assuming independent $\hat{d}_i$, $i \in \{1,\dots,4\}$, we use it for simplicity. ◇

From those assumptions and by the latter considerations we obtain the likelihood function

$$\begin{aligned} \mathcal{L}(\Theta|\hat{\mathcal{D}}) &= \mathcal{L}(\Theta|\hat{d}_1,\hat{d}_2,\hat{d}_3,\hat{d}_4) = f(\hat{d}_1,\hat{d}_2,\hat{d}_3,\hat{d}_4|\Theta) \\ &= \prod_{i=1}^{4} f_i(\hat{d}_i|\Theta) = \prod_{i=1}^{4}\frac{1}{\sqrt{(2\pi\sigma^2)^3}}\exp\left(-\frac{1}{2\sigma^2}||\hat{d}_i - d_i||_2^2\right). \end{aligned}$$

Remember that d_i, $i \in \{1,\dots,4\}$, are actually determined through Θ. Instead of maximising this function we can also minimise its negative logarithm, the so-called negative log likelihood function

$$\begin{aligned} \mathcal{J}(\Theta|\hat{\mathcal{D}}) &= -\log\mathcal{L}(\Theta|\hat{\mathcal{D}}) \\ &= 6\log(2\pi\sigma^2) + \frac{1}{2\sigma^2}\sum_{i=1}^{4}||\hat{d}_i - d_i||_2^2 \\ &= 6\log(2\pi\sigma^2) + \frac{1}{2\sigma^2}\sum_{i=1}^{4}\sum_{j=1}^{3}(\hat{\mathcal{D}}_{ij} - \mathcal{D}_{ij})^2, \end{aligned}$$

which is more convenient and better suited for numerical computations. Hence, for finding a minimiser under the given assumptions, we can equivalently use the least squares function

$$\mathcal{S}(\Theta|\hat{\mathcal{D}}) = \sum_{i=1}^{4}\sum_{j=1}^{3}(\hat{\mathcal{D}}_{ij} - \mathcal{D}_{ij})^2.$$

Due to the mismatch of amount of data and number of parameters in our case, it seems reasonable to fix some parameters before the optimisation procedure and by that reduce the number of estimated parameters in order to prevent overfitting. Following the descriptions in [25] we set the initial value of beta-lactam to $5\ \mu g\,mL^{-1}$, and assume a zero supply rate $\theta = 0\ \mu g\,mL^{-1}\,h^{-1}$. The degradation rate $\lambda = 0.2589\ h^{-1}$ is chosen such that the beta-lactam concentration is close to zero after 24 hours. Furthermore, the parameters of the logistic growth are estimated separately from general growth data of *P. aeruginosa*, which can be found in appendix A. The numerical determination of the values $r_a = 0.2946\ h^{-1}$ and $K_a = 3.1507 \times 10^7\ cells\,mL^{-1}$ is shown there as well. The starting values $T(0) = 0\ cells\,mL^{-1}$, $B(0) = 0\ cells\,mL^{-1}$, and as mentioned above $C(0) = 5\ \mu g\,mL^{-1}$ at time $t_0 = 0$ are taken from [25], whereas the initial cell density of type A is not chosen in advance.
Hence we only minimise the least squares function for the parameters ε_β, ω_1, ω_2, δ_n, and $A(0)$ by performing a multi-start optimisation, where each single optimisation is initialised with randomly sampled values for these parameters. For the evaluation of the least squares function we obviously need the theoretical data points, which we obtain by solving the ODE system and computing the proportions of the theoretical population densities at the corresponding time points. The implementation of the described optimisation procedure can be found in appendix B.

Remark 3 For optimisation we use the MATLAB function `fmincon`, which finds a minimum of a constrained non-linear multivariable function [38]. The alternative MATLAB function `fminsearch` is not appropriate for our problem since this solver returns negative parameter values. ◇

Results

The parameter values for which we obtain the closest fit to the given data are presented in table 2.3, where both fixed and estimated parameters are included.

Parameter	Meaning	Value	Unit
r_a	Intrinsic growth rate of type A	0.2946^*	h^{-1}
K_a	Carrying capacity of type A	$3.1507 \times 10^{7*}$	$cells\,mL^{-1}$
ε_β	Death rate of type A due to beta-lactam	0.1214	$mL\,h^{-1}\,\mu g^{-1}$
ω_1	Mass action coefficient for change from type A into type T	1.1675	h^{-1}
ω_2	Mass action coefficient for change from type T into type B	0.3400	h^{-1}
δ_n	Natural death rate of type B	3.5780×10^{-7}	h^{-1}
θ	Supply rate of beta-lactam	0^*	$\mu g\,mL^{-1}\,h^{-1}$
λ	Degradation rate of beta-lactam	0.2589^*	h^{-1}
$A(0)$	Initial value of type A	26.7691	$cells\,mL^{-1}$
$T(0)$	Initial value of type T	0^*	$cells\,mL^{-1}$
$B(0)$	Initial value of type B	0^*	$cells\,mL^{-1}$
$C(0)$	Initial value of beta-lactam	5^*	$\mu g\,mL^{-1}$

Table 2.3: Estimated parameter values of the Naive Model, cf. [7]. Values that were fixed before the optimisation procedure are indicated by stars.

We could not compare the estimated parameters and reason about their reliability since it was not possible to find similar models of *P. aeruginosa* in literature. However, we visualise the dynamics of the system for the estimated parameter values (figure 2.2b) and the comparison with the observed data of [25] (figure 2.2a) in order to check if the fit is meaningful. The plots in figure 2.2 are created with MATLAB using the code shown in listing 4.

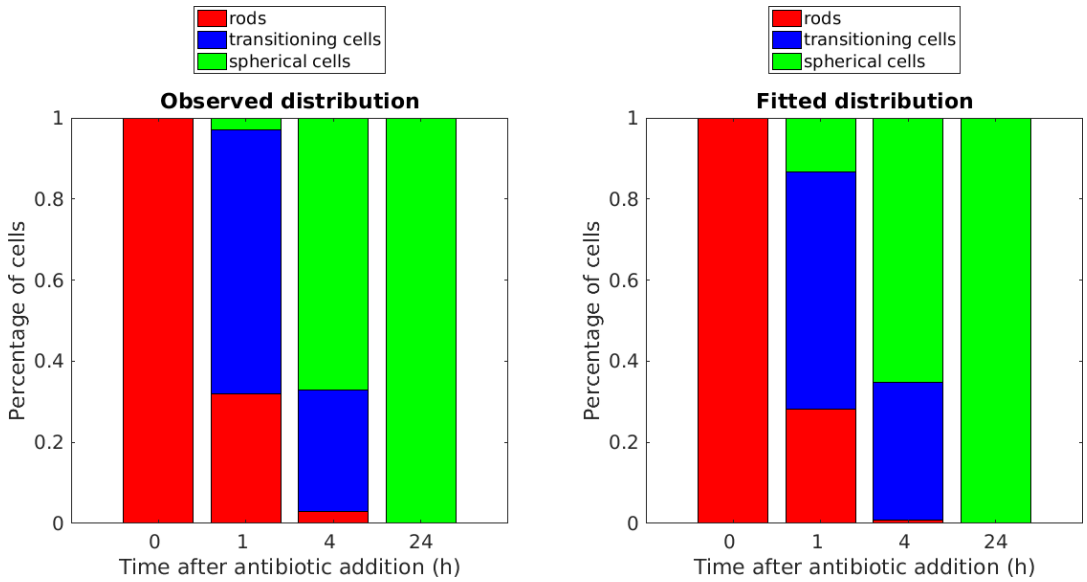

(a) Comparison of the observed (left) and the fitted data (right).

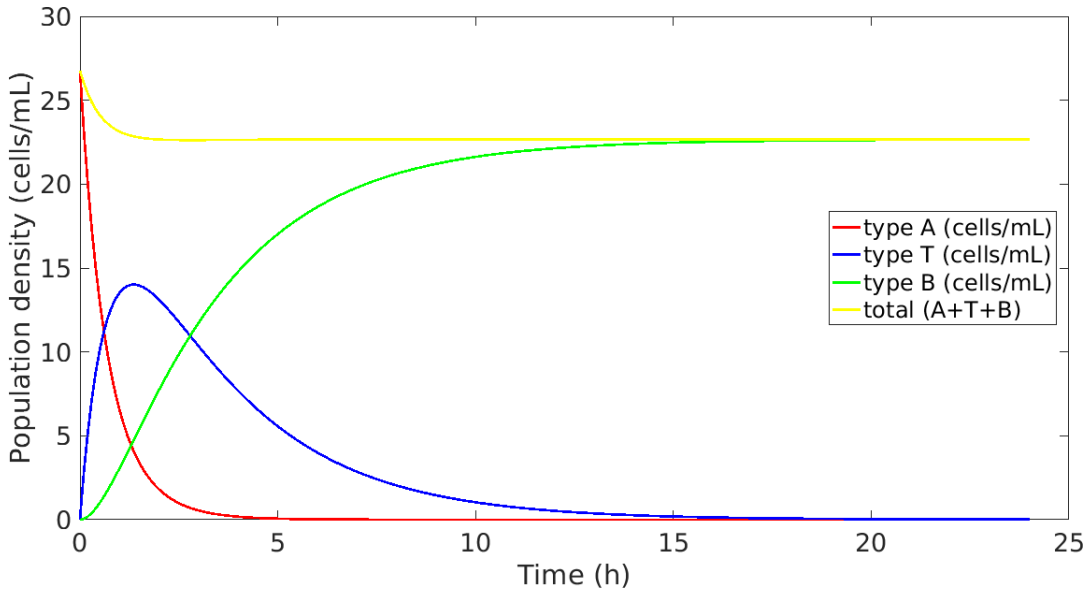

(b) Dynamics of the Naive Model for the fitted parameter values.

Figure 2.2: Comparison and dynamics for the fitted parameter values of the Naive Model.

The fit is already quite good. The proportion of spherically shaped cells after one hour in the computed data is a bit greater than the measured proportion. The calculated number of rods at the third time point is very small but at least existent.
The dynamics in figure 2.2b show the rapid conversion from rods over transitional to spherical cells. After just a few hours there are almost only spherically shaped

cells. In the long run only spherical cells are left whose density decreases since they do not reproduce. This observation will be confirmed by the analytical investigation. However, it is easier to judge the quality of the results when we later compare them with those form other models.

Uncertainty of Estimates

When performing numerical calculations, one is always interested in the quality of the results. Of course, the reliability of our numerical computations depends on the use of appropriate solvers for both the optimisation problems and the ODE systems. In MATLAB, generally steps and step sizes are controlled by these solvers themselves with preset error tolerances. One can monitor the progress of the computations and keep track of convergence, tolerances, and number of iterations among others. To obtain better results the options structure for ODE solvers can be adjusted individually by changing for instance the absolute and relative tolerances or maximum number of iterations. Moreover, there are different ODE solvers provided for specific kinds of problems like stiff and non-stiff ODEs. By using appropriate solvers, provided with additional information such as the Jacobian of the ODE system, especially the computations for stiff ODE problems can be made more efficient and reliable [33]. In appendix B we shortly discuss the solvers that were chosen for our problems. Following the suggestions in the official MATLAB documentation by The MathWorks, Inc. we obtained quite satisfying and meaningful results.
An additional option to assure the quality of the estimates is to visualise the objective function, in our case the least squares function, evaluated at different grid points of our parameter space. Estimated parameter values at a clear, visually identifiable minimum in the heatmaps in figure 2.3 and figure 2.4 indicate that they at least locally minimise the objective function, whereas the quality of fitted parameter values that are not located at a minimum in the plots is more questionable.
Since we can visualise at most three dimensions, we vary two parameters while fixing the others. The heatmaps for the mass action parameters ω_1 and ω_2 are depicted in figure 2.3. Obviously there is a local minimum at the values for ω_1 and ω_2 obtained from the optimisation. The code for generating the images can be found in listing 5. Similarly we get a picture in figure 2.4 for the parameters ε_β and δ_n. At first glance in figure 2.4a and figure 2.4b the optimised values for ε_β and δ_n seem to minimise the objective function with δ_n close to the lower boundary at zero. However, by zooming in further we see in figure 2.4c that the MATLAB determined values do not lie at a local minimum. When we reduce the optimality tolerance of the solver `fmincon`, the value for δ_n gets closer to zero. Since the estimated value of δ_n is already very small, manually setting it to the visible local minimiser $\delta_n = 0$ does hardly impact the dynamics of our model.

2.3 Mathematical Analysis

Now that we got a first impression of our model and visualised the dynamics, we are interested in concrete mathematical statements about the system like its asymptotic behaviour. Moreover, one has to guarantee positivity and boundedness for non-negative initial values in a biologically relevant model. First we determine the stationary states of the system and their stability.

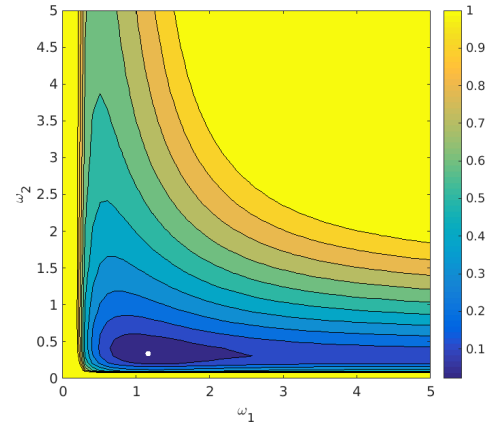

(a) $(\omega_1, \omega_2) \in [0,\ 5] \times [0,\ 5]$.

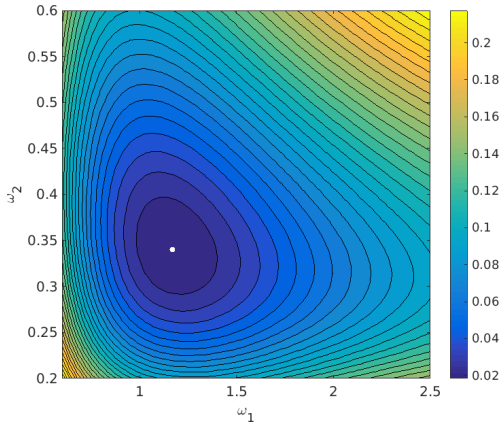

(b) $(\omega_1, \omega_2) \in [0.6,\ 2.5] \times [0.2,\ 0.6]$.

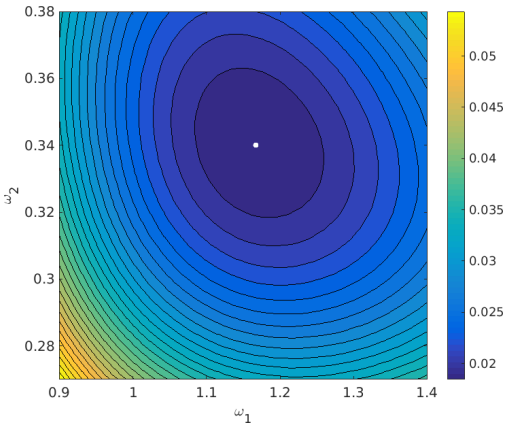

(c) $(\omega_1, \omega_2) \in [0.9,\ 1.4] \times [0.27,\ 0.38]$.

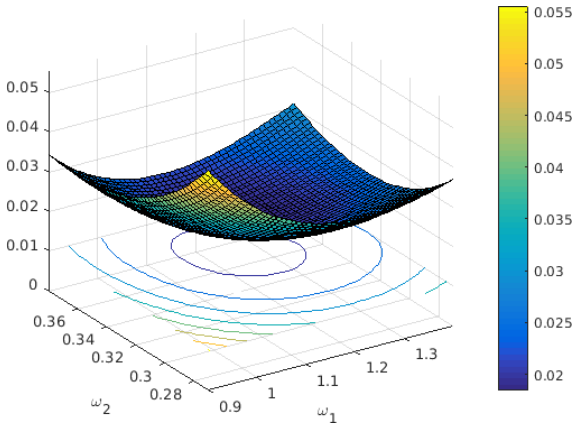

(d) Contour plot of the least squares function depending on ω_1 and ω_2.

Figure 2.3: Evaluation of the least squares function with varying parameters ω_1 and ω_2. Estimated minimum is indicated as white dot.

Stationary States

At the very beginning we need to define the concept of a "stationary state".

Definition 1 (Stationary State) *A dynamical system is said to be in a* ***stationary state*** *if it remains there as time elapses. In other words, it is a value of the state variables where they do not change anymore. Equivalent terms are "stationary point", "fixed point", or "equilibrium".*

A solution does not change anymore, if its derivative, that is the right hand side of the system, equals zero. Hence, to determine the stationary points with components

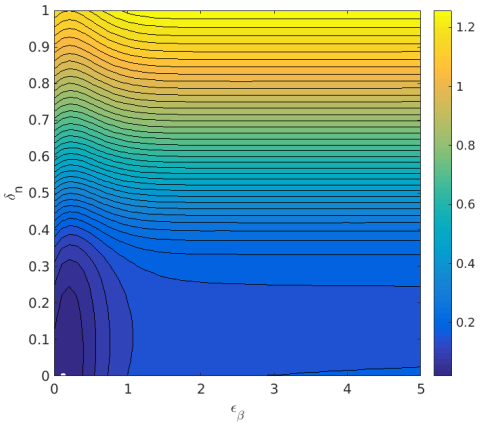

(a) $(\varepsilon_\beta, \delta_n) \in [0,\ 5] \times [0,\ 1]$.

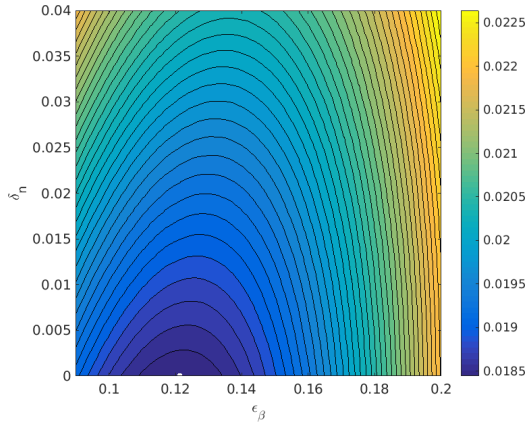

(b) $(\varepsilon_\beta, \delta_n) \in [0.09,\ 0.2] \times [0,\ 0.04]$.

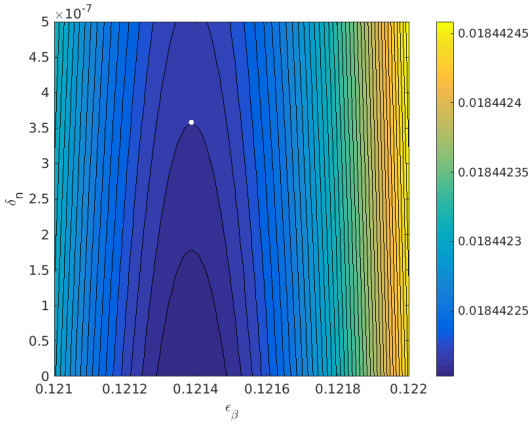

(c) $(\varepsilon_\beta, \delta_n) \in [0.121,\ 0.122] \times [0,\ 5 \times 10^{-7}]$.

Figure 2.4: Evaluation of the least squares function with varying parameters ε_β and δ_n. Estimated minimum is indicated as white dot.

A^*, T^*, B^*, and C^*, we solve the equations (2.6) to (2.9) for these variables:

$$0 = r_a A^* \left(1 - \frac{A^*}{K_a}\right) - \varepsilon_\beta A^* C^* - \omega_1 A^* \tag{2.6}$$

$$0 = \omega_1 A^* - \omega_2 T^* \tag{2.7}$$

$$0 = \omega_2 T^* - \delta_n B^* \tag{2.8}$$

$$0 = \theta - \lambda C^*. \tag{2.9}$$

Calculating by hand or solving this system by MATLAB (see listing 6) we obtain two possible fixed points

$$P_0 = (A_0^*, T_0^*, B_0^*, C_0^*) = \left(0, 0, 0, \frac{\theta}{\lambda}\right)$$

$$P_1 = (A_1^*, T_1^*, B_1^*, C_1^*) = \left(\Sigma,\ \frac{\omega_1}{\omega_2}\Sigma,\ \frac{\omega_1}{\delta_n}\Sigma,\ \frac{\theta}{\lambda}\right)$$

with

$$\Sigma := \frac{K_a(\lambda r_a - \varepsilon_\beta \theta - \lambda \omega_1)}{\lambda r_a}.$$

The point P_0 is always non-negative, and hence biologically meaningful since we assume non-negative parameters. The second point P_1 only has non-negative entries if $0 \leq \Sigma$, which is equivalent to

$$0 \leq \lambda r_a - \varepsilon_\beta \theta - \lambda \omega_1 \quad \Leftrightarrow \quad \varepsilon_\beta \frac{\theta}{\lambda} + \omega_1 \leq r_a. \tag{2.10}$$

In the case of equality in equation (2.10) the points P_0 and P_1 coincide.

Stability

We again start this section by defining the relevant term "stability" and introduce some general results for dynamical systems, before we examine the stability of the two stationary points concretely. In this section we follow in many ways the book by Müller and Kuttler [26].

For general statements we consider in the following the autonomous ODE

$$y'(t) = f(y) \tag{2.11}$$

with vector field $f \in C^1(U, \mathbb{R}^n)$, where $U \subset \mathbb{R}^n$ is a domain. Together with an initial condition $y(t_0) = y_0$, $y_0 \in U$, equation (2.11) becomes an initial value problem. Let $I \neq \emptyset$ be an interval and $y \colon I \to \mathbb{R}^n$ a solution to the initial value problem indicated by $y(t, y_0)$. We denote stationary points of f by $y^* \in \mathbb{R}^n$, i.e. $f(y^*) = 0$. The Jacobian matrix of f at the stationary point y^* is defined as $A \coloneqq f'(y^*)$, where

$$A_{ij} = \frac{\partial f_i}{\partial y_j}(y^*), \quad i, j \in \{1, \ldots, n\}.$$

Now we give a proper definition for stability, taken from [20, 26, cf. Definition 2.7 and 2.8, p. 174].

Definition 2 (Stability) *A stationary point y^* of f is called **stable** if for every neighbourhood V of y^* in U, there is a neighbourhood $V_1 \subset V$, such that every solution $y(t, y_0)$ with $y_0 \in V_1$ is defined and $y(t, y_0) \in V$ for all $t > 0$.*
*We call y^* **asymptotically stable**, if it is stable and if there is a neighbourhood V_0 of y^* in U such that for all solutions $y(t, y_0)$ with $y_0 \in V_0$, it holds $y(t) \to y^*$ for $t \to \infty$.*

For analytical purposes it is easier to consider linear instead of non-linear systems. Under certain assumptions, which will be specified in theorem 1, the linearisation of a non-linear model shows the same behaviour as the original model in a small neighbourhood of a stationary point. Therefore, we are interested in solutions $y(t)$ of equation (2.11) and their behaviour in a neighbourhood of y^*, i.e. $y(t) = y^* + z(t)$ for small $z(t)$, yielding

$$z'(t) = y'(t) = f(y^* + z(t)) = \underbrace{f(y^*)}_{=0} + f'(y^*)z(t) + o(||z(t)||),$$

where we used Taylor expansion. Hence, by approximating with linear terms we obtain the corresponding linearised system

$$z'(t) = Az(t).$$

Another tool to analyse stability in non-linear systems are Lyapunov functions, cf. [26, 2]. However, we stick to the former approach and apply proposition 1 and theorem 1.

Proposition 1 (Stability) *Let $f \in C^1(U, \mathbb{R}^n)$ and let y^* be a stationary point of f. We denote the spectrum of $A = f'(y^*)$ by $\sigma(A)$.*
If the real parts of all eigenvalues of A are negative, i.e.

$$\mathrm{Re}(\sigma(A)) < 0,$$

then y^* is asymptotically stable.
Moreover, $\mathrm{Re}(\sigma(A)) \cap (0, \infty) \neq \emptyset$ implies that y^* is unstable [2, 26].

Remark 4 It is possible to be more precise under the assumptions of proposition 1: y^* is even exponentially asymptotically stable. If $\mathrm{Re}(\sigma(A)) < \alpha < 0$, then there are constants δ, $C > 0$, such that $||y(0) - y^*|| < \delta$ implies $||y(t) - y^*|| < Ce^{\alpha t}$ for $t > 0$, cf. [2, 26]. ◇

Linearisation can only be used for the analysis of local behaviour, and additional restrictions apply when statements about non-linear models and their linearisations correspond. This is captured by definition 3 and theorem 1, taken from [26, Definition 2.18 and Theorem 2.19, p. 208].

Definition 3 (Hyperbolic stationary point) *A stationary point y^* is called **hyperbolic** if $0 \notin \mathrm{Re}(\sigma(f'(y^*)))$.*

Theorem 1 (Hartman-Grobman) *Let y^* be a hyperbolic stationary point. Then there is a neighbourhood U of y^* and a homeomorphism $H : U \to \mathbb{R}^n$ with $H(y^*) = 0$, which maps the trajectories of $y'(t) = f(y)$ one-to-one into trajectories of the linearised system $z'(t) = Az(t)$, with respect to the time course.*

For further discussion and an outline of the proof of the Hartman-Grobman Theorem we refer to [30, Section 2.8, p. 118ff].

We now apply the general results to our system. The right hand side of our system is continuously differentiable, hence the Jacobian at a point $P = (A(t), T(t), B(t), C(t))$

can be derived as

$$J(P) = \begin{pmatrix} r_a - 2\frac{r_a}{K_a}A(t) - \varepsilon_\beta C(t) - \omega_1 & 0 & 0 & -\varepsilon_\beta A(t) \\ \omega_1 & -\omega_2 & 0 & 0 \\ 0 & \omega_2 & -\delta_n & 0 \\ 0 & 0 & 0 & -\lambda \end{pmatrix}.$$

This matrix J evaluated at the stationary point P_0 gives the matrix

$$J_0 \coloneqq J(P_0) = \begin{pmatrix} r_a - \varepsilon_\beta \frac{\theta}{\lambda} - \omega_1 & 0 & 0 & 0 \\ \omega_1 & -\omega_2 & 0 & 0 \\ 0 & \omega_2 & -\delta_n & 0 \\ 0 & 0 & 0 & -\lambda \end{pmatrix}.$$

Since J_0 is a lower triangular matrix, we directly obtain the four eigenvalues

$$-\lambda,\ -\delta_n,\ -\omega_2, \text{ and } r_a - \varepsilon_\beta \frac{\theta}{\lambda} - \omega_1.$$

Theorem 1 can be applied if λ, δ_n, $\omega_2 \neq 0$ and $r_a \neq \varepsilon_\beta\theta/\lambda + \omega_1$. Since we assume non-negative parameter values, it follows that the stationary point $P_0 = (0, 0, 0, \theta/\lambda)$ is asymptotically stable if and only if $r_a < \varepsilon_\beta\theta/\lambda + \omega_1$. Biologically this means that the population goes extinct if the intrinsic growth rate is smaller than the rates for mass action and death caused by beta-lactam (multiplied by the ratio of antibiotic supply). In the case of our parameter values P_0 is stable, i.e. the bacteria population dies out.
For the second stationary point $P_1 = (\Sigma,\ \Sigma\omega_1/\omega_2,\ \Sigma\omega_1/\delta_n,\ \theta/\lambda)$ we obtain the Jacobian

$$J_1 \coloneqq J(P_1) = \begin{pmatrix} -r_a + \varepsilon_\beta \frac{\theta}{\lambda} + \omega_1 & 0 & 0 & \frac{\varepsilon_\beta K_a(-\lambda r_a + \varepsilon_\beta\theta + \lambda\omega_1)}{\lambda r_a} \\ \omega_1 & -\omega_2 & 0 & 0 \\ 0 & \omega_2 & -\delta_n & 0 \\ 0 & 0 & 0 & -\lambda \end{pmatrix}.$$

Using for example Laplace's formula and expanding along the third column we get the corresponding eigenvalues

$$-\lambda,\ -\delta_n,\ -\omega_2, \text{ and } -r_a + \varepsilon_\beta \frac{\theta}{\lambda} + \omega_1.$$

With the same argumentation theorem 1 tells us that the point is asymptotically stable if and only if λ, δ_n, and ω_2 are positive and $\varepsilon_\beta\theta/\lambda + \omega_1 < r_a$. Together with the considerations at the beginning of this subsection in (2.10), we know that P_1 is stable as long as it is biologically relevant and not equal to P_0.
This corresponds to a transcritical bifurcation. If $r_a < \varepsilon_\beta\theta/\lambda + \omega_1$, P_0 is stable and P_1 does not exist in a biologically meaningful way. In contrast, if $r_a > \varepsilon_\beta\theta/\lambda + \omega_1$, P_0 looses its stability and instead P_1 appears to be relevant and stable. Thus, the critical point is at

$$r_a = \varepsilon_\beta \frac{\theta}{\lambda} + \omega_1, \tag{2.12}$$

where P_0 equals P_1 and stability interchanges.
We consider this bifurcation now for our parameter values. Since $\theta = 0$, stability

interchanges when $r_a = \omega_1$. To visualise the stability areas, we plot r_a as a function of ω_1, which in our case is just the identity:

$$r_a(\omega_1) = \varepsilon_\beta \frac{\theta}{\lambda} + \omega_1 = \omega_1.$$

The stability areas are shown in figure 2.5a.
Alternatively we can solve equation (2.12) for θ and leave r_a, λ, and ε_β fix, which leads to the function

$$\theta(\omega_1) = (r_a - \omega_1)\frac{\lambda}{\varepsilon_\beta}.$$

The stability areas for the two stationary points are plotted in figure 2.5b. The plot also reveals the critical point where $r_a = \omega_1$ and θ turns negative afterwards, which is biological not meaningful anymore. Hence, for parameter values for which $\omega_1 > r_a$ holds, only P_0 is stable.

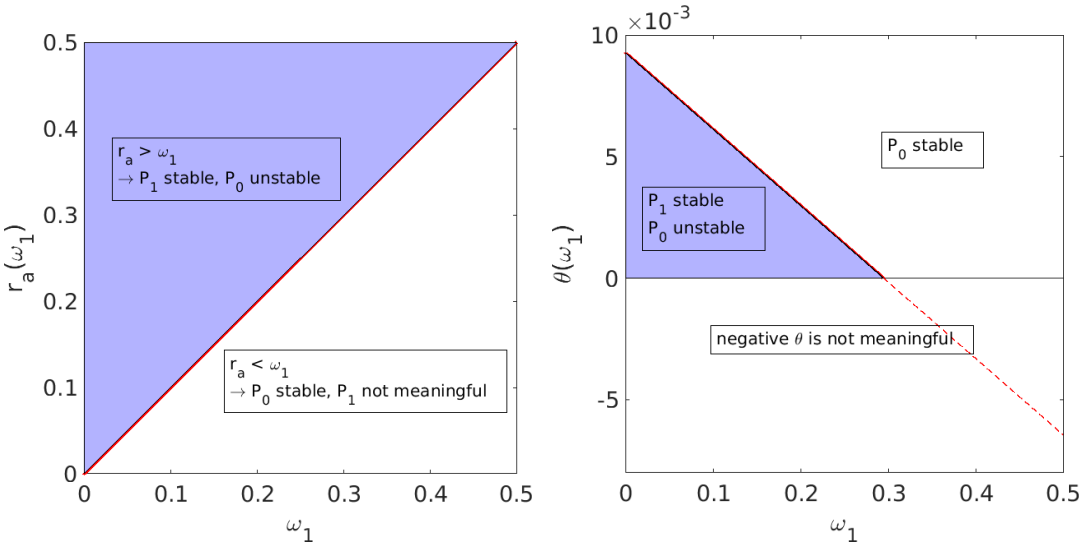

(a) If $r_a > \omega_1$, P_1 is stable. If $r_a < \omega_a$, P_0 is stable.

(b) If $0 < \theta < \theta(\omega_1)$, P_1 is stable. If $\theta > \theta(\omega_1)$, P_0 is stable. When ω_1 reaches the value of r_a at 0.2946, $\theta(\omega_1)$ turns negative, which is biologically not meaningful anymore.

Figure 2.5: Stability areas for the two stationary points depending on different parameter values and their relations.

Additionally we check whether the behaviour of the numerical solution of the ODE system (2.1) to (2.4) for different values of ω_1 corresponds to the considerations above. Therefore, we look where the population densities tend to in the long run when the ODE system is solved for the estimated parameter values but with ω_1 changing between zero and $0.5\ \mathrm{h}^{-1}$. The population densities of the different cell types after 500 hours are depicted in figure 2.6a. The plot confirms the previous considerations: there exists a non-trivial point as long as $\omega_1 < r_a$, which corresponds to the coexistence point P_1 in that region. When ω_1 reaches and exceeds r_a there are no cells left, which is compatible to the stationary point P_0 for those parameter values. Note that it is possible that the concentration of cells of type B exceeds the carrying capacity $K_a = 3.1507 \times 10^7\ \mathrm{cells\,mL}^{-1}$ of rod shaped cells. We later derive the bound $\omega_1 K_a/\delta_n$ for cells of type B, which for our parameter values equals

$1.0281 \times 10^{14}\,\text{cells}\,\text{mL}^{-1}$.
Finally we visualise the stationary point P_1 as a function of ω_1 in figure 2.6b by plotting the population densities of the three cell types against ω_1. Also here we see that the coexistence point with a high concentration of type B cells is meaningful when $\omega_1 < r_a$, but it becomes biologically irrelevant when the critical point is reached since then the population density of type B cells turns negative.

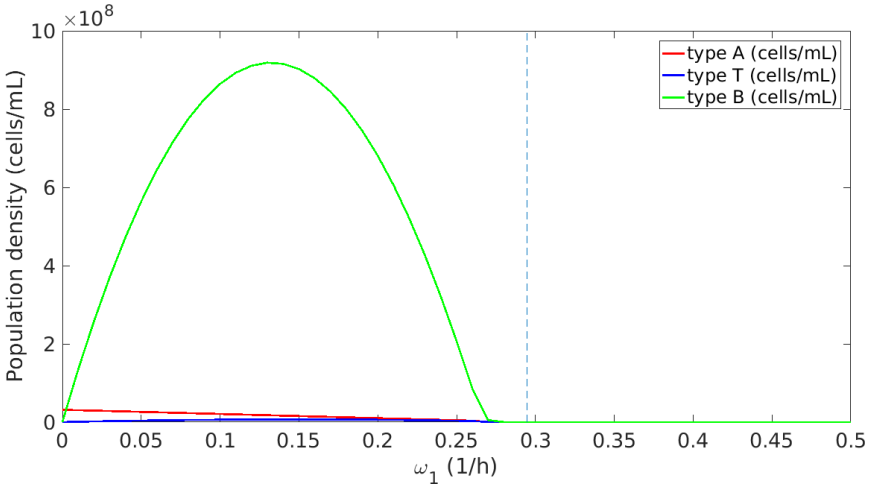

(a) Population densities of the numerical solution after 500 hours with varying values of ω_1.

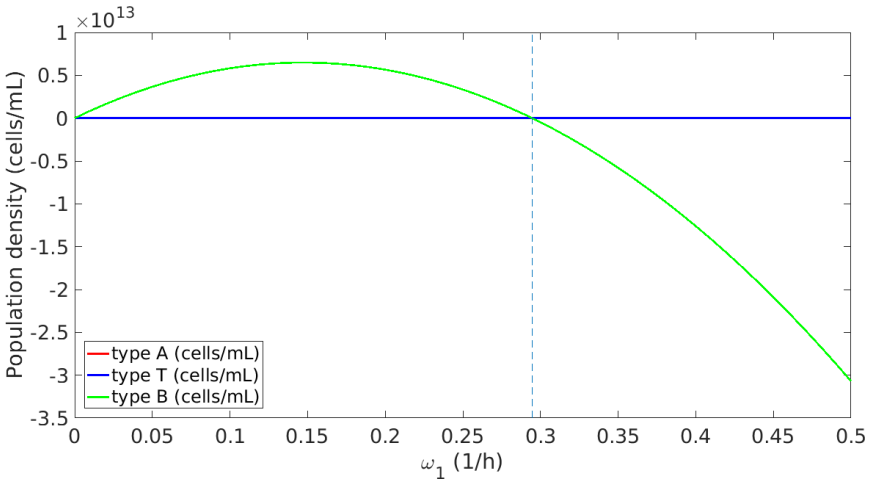

(b) Population densities in the stationary point P_1 for different values of ω_1. The components A_1^* and T_1^* of P_1 are not distinguishable since B_1^* is very large in comparison.

Figure 2.6: Population densities for different values of ω_1. The dashed line indicates the critical point where ω_1 equals r_a. Listing 7 generates the plot.

Positivity

Another important aspect for the biological relevance of our model is that the whole system stays positive. In our case this means to show that $\mathbb{R}^4_+$ is positively invariant, i.e. starting in the positive domain, $y(t_0) = y_0 \in \mathbb{R}^4_+$, the solution $y(t, y_0)$ stays there for $t > t_0$. As in the section for stability, we state a helpful, general proposition

about the positivity of a dynamical system, which is taken from [35, Proposition B.7, p. 267].

Proposition 2 (Positivity) *Suppose that f in (2.11) has the following two properties:*

- *solutions $y(t, y_0)$ of initial value problems $y(t_0) = y_0 \geq 0$ are unique, and*
- *whenever $y(t) \geq 0$ satisfies $y_i(t) = 0$, it holds $f_i(y) \geq 0$ for all $i \in \{1, \ldots, n\}$.*

Then, provided that $y(t_0) \geq 0$, it follows $y(t) \geq 0$ for all $t \geq t_0$ for which it is defined.

Generally, if we write an inequality concerning a vector, e.g. $y(t) \geq 0$, the relation is meant component-by-component. The proof of this proposition can be found in [35]. For showing uniqueness of a solution one can make use of the theorem by Picard-Lindelöf:

Theorem 2 (Picard-Lindelöf) *Consider the initial value problem*

$$y'(t) = f(y), \quad y(t_0) = y_0,$$

as in (2.11). If f is uniformly Lipschitz-continuous in its domain of definition U and $y_0 \in U$, then there exist an $\varepsilon > 0$ and a unique solution $y \colon [t_0 - \varepsilon, t_0 + \varepsilon] \to \mathbb{R}^n$ of the initial value problem with $graph(y) \subset U$.

We need to check the assumptions of theorem 2. Obviously the right hand side of the system (2.1) to (2.4) is continuously differentiable and hence also Lipschitz-continuous with respect to $(A(t), T(t), B(t), C(t))$. This means that there exists a locally unique solution as required in the proposition.
It remains to show that for any $y = (y_1, y_2, y_3, y_4) \coloneqq (A(t), T(t), B(t), C(t)) \geq 0$ with $y_i = 0$, it holds $f_i(y) \geq 0$, where f_i denotes the corresponding vector field for y_i, $i \in \{1, \ldots, 4\}$. Let $A(t)$, $T(t)$, $B(t)$, $C(t)$ be non-negative.

- If $A(t) = 0$, then

$$\frac{dA}{dt}(t) = r_a A(t) \left(1 - \frac{A(t)}{K_a}\right) - \varepsilon_\beta A(t) C(t) - \omega_1 A(t) = 0 \geq 0.$$

- If $T(t) = 0$, then

$$\frac{dT}{dt}(t) = \omega_1 A(t) - \omega_2 T(t) = \omega_1 A(t) \geq 0.$$

- If $B(t) = 0$, then

$$\frac{dB}{dt}(t) = \omega_2 T(t) - \delta_n B(t) = \omega_2 T(t) \geq 0.$$

- If $C(t) = 0$, then

$$\frac{dC}{dt}(t) = \theta - \lambda C(t) = \theta \geq 0.$$

Hence, we know by proposition 2 that the solution stays positive if we start in the positive domain.

Boundedness

Since population densities are naturally bounded from above, we finally investigate whether our model satisfies this property. To show that the solution does not tend to infinity for positive initial values, we derive an upper bound for each variable. Therefore, we transform the system appropriately to be able to apply proposition 2. First we show that $A(t)$ cannot exceed the carrying capacity K_a. To this end we define the new variable $X(t) \coloneqq K_a - A(t)$. By replacing $A(t)$ in the original system by $X(t)$, the transformed system consists of the derivative of the new variable

$$\begin{aligned}\frac{dX}{dt}(t) &= -\frac{dA}{dt}(t) = -r_a A(t)\left(1 - \frac{A(t)}{K_a}\right) + \varepsilon_\beta A(t)C(t) + \omega_1 A(t) \\ &= -\frac{r_a}{K_a}X(t)(K_a - X(t)) + \varepsilon_\beta (K_a - X(t))C(t) + \omega_1(K_a - X(t)),\end{aligned}$$

the adapted differential equation for $T(t)$

$$\frac{dT}{dt}(t) = \omega_1 A(t) - \omega_2 T(t) = \omega_1(K_a - X(t)) - \omega_2 T(t),$$

and the unchanged equations for $B(t)$ and $C(t)$. We now apply proposition 2. Since the original system has a locally unique solution, this also exists for the transformation. For the second condition of the proposition we need a non-negative derivative of $X(t)$ if $X(t) = 0$ and $T(t)$, $B(t)$, and $C(t)$ are non-negative. It holds

$$\frac{dX}{dt}(t) = \varepsilon_\beta K_a C(t) + \omega_1 K_a \geq 0.$$

Now we consider the derivative of $T(t)$ with $T(t) = 0$ and non-negative $B(t)$, $C(t)$, and $X(t)$:

$$\frac{dT}{dt}(t) = \omega_1(K_a - X(t)) - \omega_2 T(t) = \omega_1(K_a - X(t)) \geq 0,$$

if we assume that $K_a - X(t)$ is non-negative, which is equivalent to assume a non-negative $A(t)$. Since the differential equations of $B(t)$ and $C(t)$ do not depend on $A(t)$ in the original system, their derivatives in the transformed system still satisfy the non-negativity condition of proposition 2. By this proposition it follows that if $0 \leq A(0) \leq K_a$, then $X(t) \geq 0$ which is equivalent to $A(t) \leq K_a$. Hence K_a is an upper bound for the variable $A(t)$.
One can proceed in the same way for the variables $T(t)$, $B(t)$, and $C(t)$ by transforming them and applying proposition 2 to the new systems. It can be shown that $\omega_1 K_a/\omega_2$ is an upper bound for $T(t)$, $\omega_1 K_a/\delta_n$ an upper bound for $B(t)$, and θ/λ one for $C(t)$.
Note that in general if the initial value lies above the indicated bound, then the derivative of the solution surely is negative at least until the bound is reached. In that case the bound has to be adjusted appropriately by the initial value.

Boundedness can also be used to deduce another important mathematical property of the solution. Therefore, we need definition 4 of a maximal solution, taken from [20].

Definition 4 (Maximal Solution) *A solution $y\colon I \to \mathbb{R}^n$ of the initial value problem (2.11) is called maximal, if there is no solution $z\colon J \to \mathbb{R}^n$ with $I \subset J$ and $z_{|I} = y$. The interval I is open: $I = (a, b)$.*

With the help of Zorn's lemma one can show the existence of a maximal solution of the initial value problem (2.11). Proposition 3 specifies a condition when the maximal solution is also a global solution, see [20, 30].

Proposition 3 *We consider the initial value problem (2.11). Let $U = \mathbb{R}^n$, $y_0 \in U$, and let $y\colon (a, b) \to \mathbb{R}^n$ be the maximal solution. If $b = \infty$, then the solution exists for all $t > t_0$. If $b < \infty$, it holds*

$$||y(t)|| \to \infty \quad \text{for } t \to b_-.$$

By theorem 2 we obtain a unique solution on an interval $[t_0 - \varepsilon, t_0 + \varepsilon]$, which can be extended to a maximal solution on an interval $[\sigma_-, \sigma_+]$. By the boundedness of our solution, we know that $||y(t)||$ does not tend to infinity and proposition 3 tells us that the upper bound σ_+ cannot be finite. It follows the global unique existence of the solution of the ODE system.

2.4 Modification of the Naive Model

Before setting up a different model in chapter 3, we first vary the underlying growth model of *P. aeruginosa* by replacing the logistic growth by a nutrient dependent growth. We already fitted the parameter values of the nutrient dependent growth model in appendix A. The dynamics are described by equations (2.13) to (2.17).

$$\frac{dA}{dt}(t) = \underbrace{r_a A(t)\left(\frac{N(t)^n}{K_N^n + N(t)^n}\right)}_{\text{nutrient dep. growth}} - \underbrace{\varepsilon_\beta A(t)C(t)}_{\text{death by beta-lactam}} - \underbrace{\omega_1 A(t)}_{\text{conversion to } T} \tag{2.13}$$

$$\frac{dT}{dt}(t) = \underbrace{\omega_1 A(t)}_{\text{conversion to } T} - \underbrace{\omega_2 T(t)}_{\text{conversion to } B} \tag{2.14}$$

$$\frac{dB}{dt}(t) = \underbrace{\omega_2 T(t)}_{\text{conversion to } B} - \underbrace{\delta_n B(t)}_{\text{natural death}} \tag{2.15}$$

$$\frac{dC}{dt}(t) = \underbrace{\theta}_{\text{supply}} - \underbrace{\lambda C(t)}_{\text{degradation}} \tag{2.16}$$

$$\frac{dN}{dt}(t) = \underbrace{DN_0}_{\text{nutrient supply}} \underbrace{- \psi A(t)\left(\frac{N(t)^n}{K_N^n + N(t)^n}\right)}_{\text{nutrient uptake}} \tag{2.17}$$

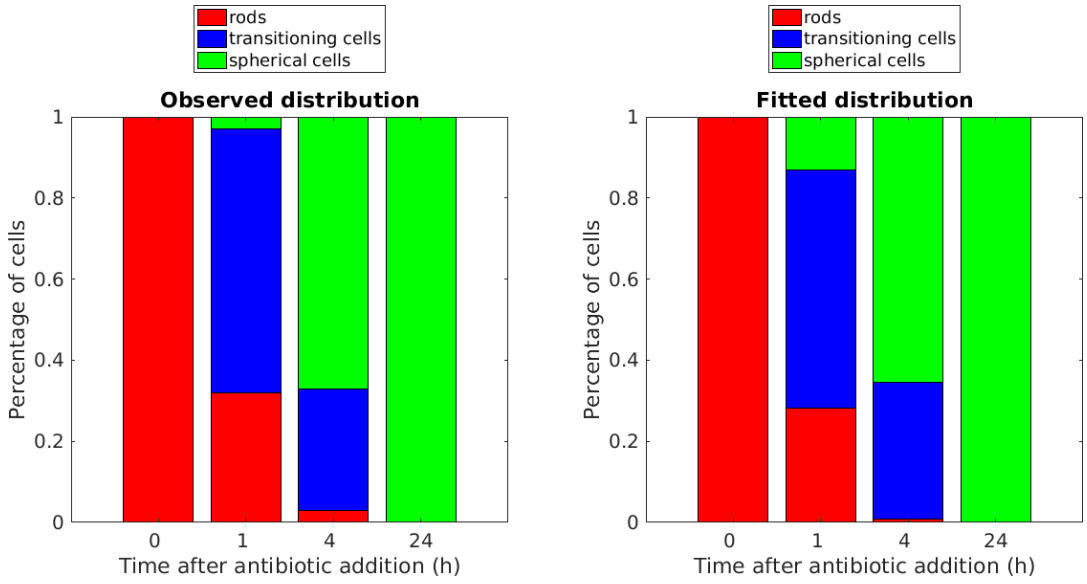

Figure 2.7: Comparison of the observed (left) and the fitted data (right) from the modification of the Naive Model.

The description and parameters regarding the growth term and equation (2.17) can be found in appendix A. The bar charts in figure 2.7 look similar to the original Naive Model. Since the system has one more equation and hence also more parameters and degrees of freedom respectively, the value of the least squares function is slightly smaller for the modification.

2.5 Reversion

As described in chapter 1, *P. aeruginosa* revert to their normal rod shape when beta-lactam is washed out. To model this phenomenon we mostly use the previous notation and variables but introduce two different parameters for the mass action of reversion: transition from type B back to type T takes place with mass action rate ξ_1, whereas ξ_2 denotes the rate for mass action from T to A.
Equations (2.18) to (2.20) represent a simple model for the reversion.

$$\frac{dA}{dt}(t) = \underbrace{r_a A(t)\left(1 - \frac{A(t)}{K_a}\right)}_{\text{log. growth}} + \underbrace{\xi_2 T(t)}_{\text{conversion to } A} \tag{2.18}$$

$$\frac{dT}{dt}(t) = \underbrace{\xi_1 B(t)}_{\text{conversion to } T} - \underbrace{\xi_2 T(t)}_{\text{conversion to } A} \tag{2.19}$$

$$\frac{dB}{dt}(t) = -\underbrace{\xi_1 B(t)}_{\text{conversion to } T} - \underbrace{\delta_n B(t)}_{\text{natural death}} \tag{2.20}$$

For parameter fitting we proceed as before using the observed data in figure 1.4b. The estimated parameter values are presented in table 2.4.

Parameter	Meaning	Value	Unit
r_a	Intrinsic growth rate of type A	0.2946^*	h^{-1}
K_a	Carrying capacity of type A	$3.1507 \times 10^{7*}$	$\mathrm{cells\,mL}^{-1}$

Parameter	Meaning	Value	Unit
ξ_1	Mass action coefficient for change from type B into type T	0.1256	h^{-1}
ξ_2	Mass action coefficient for change from type T into type A	0.3265	h^{-1}
δ_n	Natural death rate of type B	0.9202	h^{-1}
$A(0)$	Initial value of type A	0^*	$\mathrm{cells\,mL}^{-1}$
$T(0)$	Initial value of type T	0^*	$\mathrm{cells\,mL}^{-1}$
$B(0)$	Initial value of type B	73.1962	$\mathrm{cells\,mL}^{-1}$

Table 2.4: Estimated parameter values of the Reversion Model, cf. [7]. Values that were fixed before the optimisation procedure are indicated by stars.

The respective plots of the dynamics and the comparison to the original data in figure 1.4b for the initial population densities in table 2.4 are shown in figure 2.8.
The result is quite satisfying, even though the proportions of spherical and transitioning cells after 6h are a bit different than in [25]. As expected the dynamics show that the spheres rapidly convert back into transitioning and rod cells, which themselves start to reproduce new cells. This leads to the strong increase of the total population density, which after some hours solely exists of rods.
We leave out an in-depth analytical examination of the system since this works similarly as for the first part, but we make the note that the system stays positive and possesses the stationary points $(0, 0, 0)$ and $(K_a, 0, 0)$. In our case, the latter one is stable, whereas the first is not, meaning that the bacterial population will remain and grow up to the natural limit.
One could also merge the models for conversion and reversion but this would not give many new insights or a deeper understanding. Therefore, we pass over to start introducing the second approach where we model the observations by explaining the conversion with the help of QS.

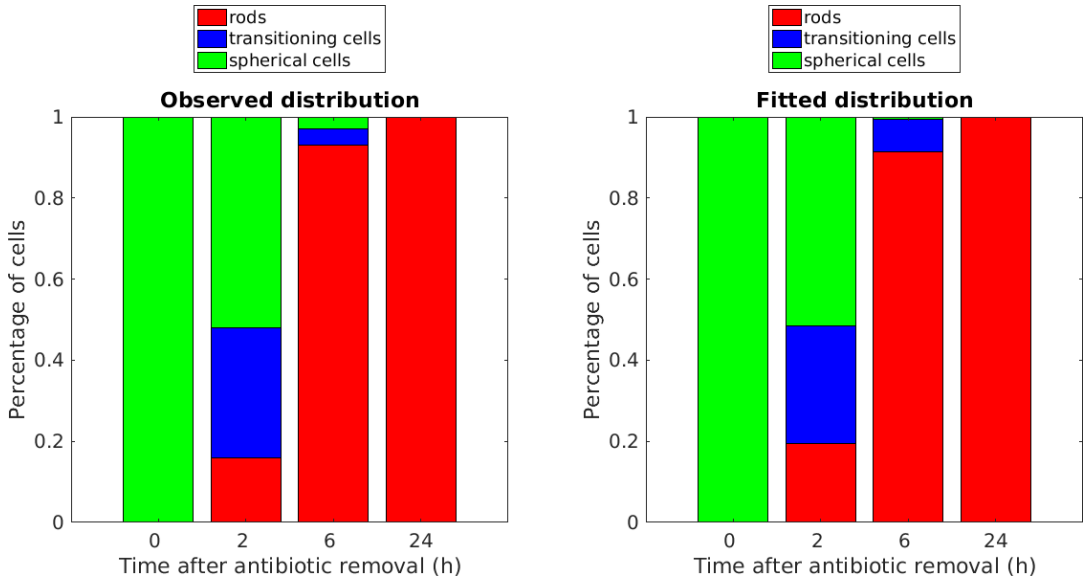

(a) Comparison of the observed (left) and the fitted data (right).

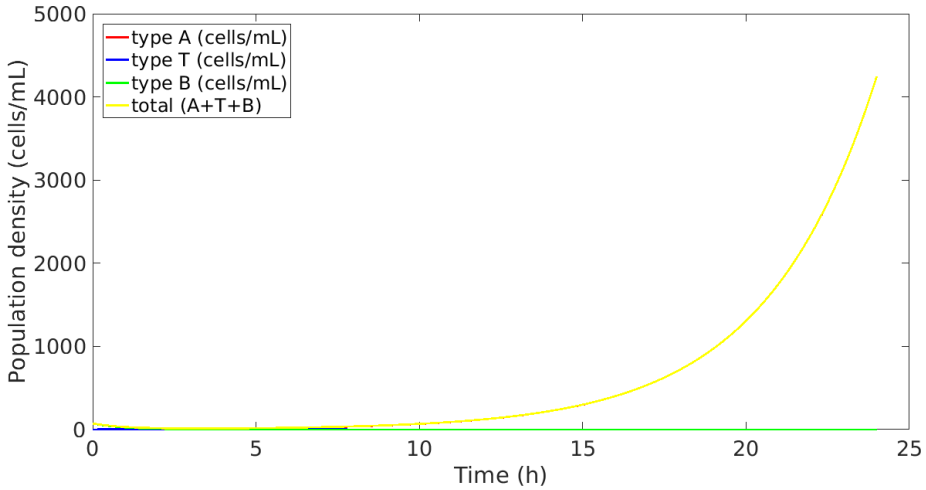

(b) Dynamics of the Reversion Model over 24h for the fitted parameter values.

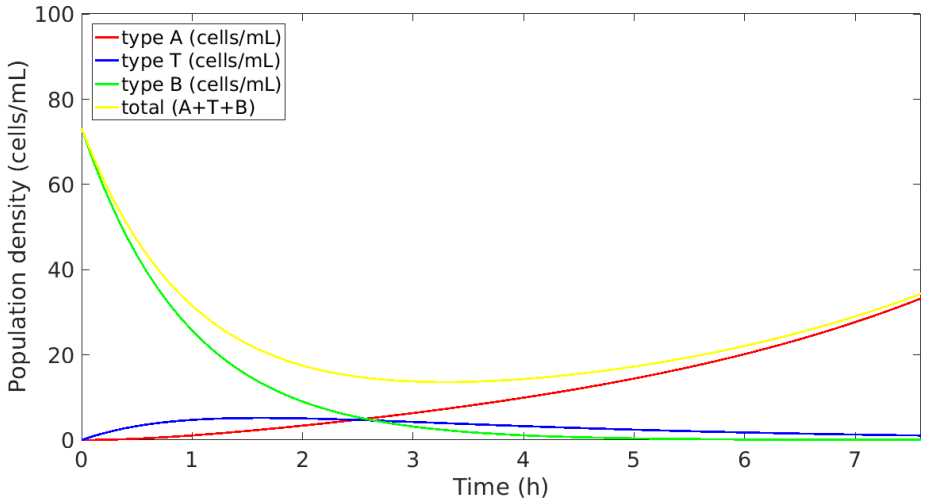

(c) Dynamics of the Reversion Model in the first seven hours.

Figure 2.8: Comparison and dynamics for the fitted parameter values of the Reversion Model.

The QS Model

In this chapter we model the conversion of *P. aeruginosa* from rods to spherically shaped cells by explaining it with QS. We extend the Naive Model by assuming that the signal molecules produced in the QS system induce the change in shape, and add the concentration of those as an additional variable.

3.1 Model Variables, Assumptions, and Parameters

Model Variables

The different types of bacteria stay the same as in the Naive Model: type A represents *P. aeruginosa* in their natural rod shape, type T denotes transitioning cells, and type B represents cells after transformation into a spherical shape. The notations for the corresponding population densities $A(t)$, $T(t)$, and $B(t)$ of the different types at time t also remain the same. Similarly, $C(t)$ denotes again the concentration of beta-lactam antibiotics in the system at time t. Additionally, a new variable for the concentration of QS signal molecules at time t comes into play, which is denoted by $S(t)$.
Hence, table 2.1 is enlarged by the latter variable and we obtain table 3.1.

Variable	Meaning	Unit
$A(t)$	Population density of *P. aeruginosa* of type A (natural rod shape)	$\mathrm{cells\,mL^{-1}}$
$T(t)$	Population density of *P. aeruginosa* of type T (transitioning shape)	$\mathrm{cells\,mL^{-1}}$
$B(t)$	Population density of *P. aeruginosa* of type B (spherical shape)	$\mathrm{cells\,mL^{-1}}$
$C(t)$	Concentration of beta-lactam	$\mathrm{\mu g\,mL^{-1}}$
$S(t)$	Concentration of QS signal molecules	$\mathrm{\mu g\,mL^{-1}}$

Table 3.1: Variables of the QS Model, cf. [7].

Assumptions and Model Parameters

In this model we build on the assumptions in section 2.1. Since we now assume that the conversion is induced by QS signal molecules, we need to change the term for mass action from type A to type T depending on the concentration of signal molecules $S(t)$. Mass action from type T into B is supposed to take place automatically assuming that transitioning cells have the intrinsic property to change their shape. The dynamics of $S(t)$ depend on the production and degradation of signal molecules. Their concentration is reduced according to some degradation rate γ. Following [7], we assume that the production takes place at a constant rate μ and

is augmented by the so-called autoinduction, which describes the phenomenon that the production rate of signal molecules increases with increasing bacterial cell density. Autoinduction is modelled by the term $\nu S(t)A(t)/(K + S(t))$, where ν is the maximum rate of production of signal molecules due to autoinduction and K denotes the half saturation constant, i.e. the value at which half the maximum rate is reached. We assume that signal molecules are only produced when antibiotics are existent in the system, as response to environmental stress, i.e. the concentration $C(t)$ affects the production. Later we will modify this assumption by modelling permanent autoinduction which then is increased under presence of antibiotics.

For now, the dynamics are modelled by the following equations (3.1) to (3.5).

$$\frac{dA}{dt}(t) = \underbrace{r_a A(t)\left(1 - \frac{A(t)}{K_a}\right)}_{\text{log. growth}} - \underbrace{\varepsilon_\beta A(t)C(t)}_{\text{death by beta-lactam}} - \underbrace{\omega_1 A(t)S(t)}_{\text{conversion to } T} \tag{3.1}$$

$$\frac{dT}{dt}(t) = \underbrace{\omega_1 A(t)S(t)}_{\text{conversion to } T} - \underbrace{\omega_2 T(t)}_{\text{conversion to } B} \tag{3.2}$$

$$\frac{dB}{dt}(t) = \underbrace{\omega_2 T(t)}_{\text{conversion to } B} - \underbrace{\delta_n B(t)}_{\text{natural death}} \tag{3.3}$$

$$\frac{dC}{dt}(t) = \underbrace{\theta}_{\text{supply}} - \underbrace{\lambda C(t)}_{\text{degradation}} \tag{3.4}$$

$$\frac{dS}{dt}(t) = \underbrace{\left(\mu + \frac{\nu S(t)}{K + S(t)}\right) A(t)C(t)}_{\text{production with autoinduction}} - \underbrace{\gamma S(t)}_{\text{degradation}} \tag{3.5}$$

The model setting is visualised in figure 3.1.

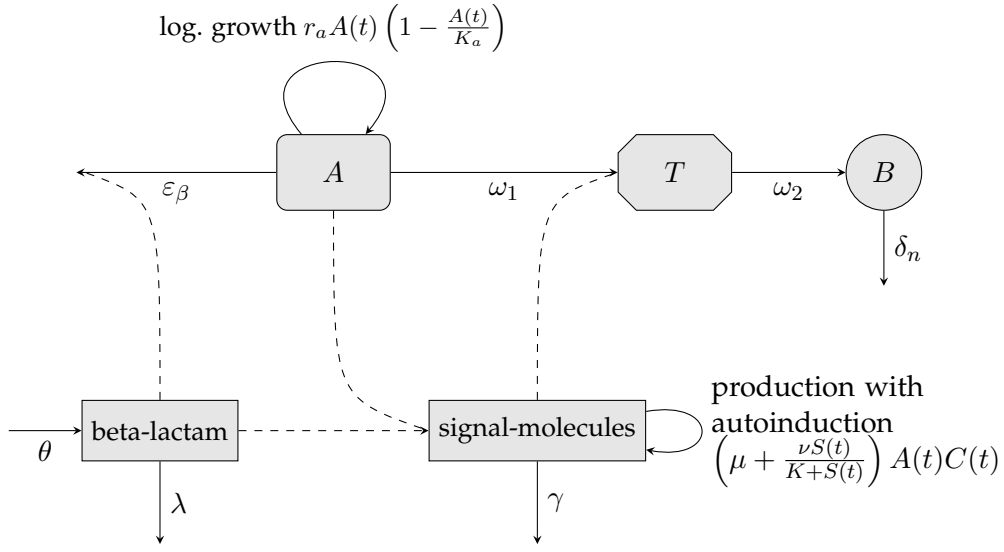

Figure 3.1: Flow diagram of the QS Model.

Table 3.2 gives an overview of the model parameters together with their units.

Parameter	Meaning	Unit
r_a	Intrinsic growth rate of type A	h^{-1}
K_a	Carrying capacity of type A	$\mathrm{cells\,mL}^{-1}$
ε_β	Death rate of type A due to beta-lactam	$\mathrm{mL\,h}^{-1}\,\mu\mathrm{g}^{-1}$
ω_1	Mass action coeff. for change from type A into type T	$\mathrm{mL\,h}^{-1}\,\mu\mathrm{g}^{-1}$
ω_2	Mass action coeff. for change from type T into type B	h^{-1}
δ_n	Natural death rate of type B	h^{-1}
θ	Supply rate of beta-lactam	$\mu\mathrm{g\,mL}^{-1}\,\mathrm{h}^{-1}$
λ	Degradation rate of beta-lactam	h^{-1}
μ	Signal production coefficient	$\mathrm{mL\,cells}^{-1}\,\mathrm{h}^{-1}$
ν	Maximum rate of production of signal molecules due to autoinduction	$\mathrm{mL\,cells}^{-1}\,\mathrm{h}^{-1}$
K	Half saturation constant for autoinduction	$\mu\mathrm{g\,mL}^{-1}$
γ	Degradation rate of signal molecules	h^{-1}

Table 3.2: Parameters of the QS Model, cf. [7].

3.2 Parameter Fitting and Evaluation

Similar to chapter 2 we fit the different parameters in order to test whether the model of equations (3.1) to (3.5) is able to explain the biological observations. The computational procedure is the same as before just that we fit more parameters this time: besides the mass action parameters ω_1 and ω_2 and death rates ε_β and δ_n, we also need to find values for the parameters μ, ν, and K in equation (3.5). Additionally we leave the initial values for cells of type A and for signal molecules open and fit also these values. In contrast, the parameters we fixed for the Naive Model are again chosen in advance and their values are kept. Concretely this means $T(0) = 0\ \mathrm{cells\,mL}^{-1}$, $B(0) = 0\ \mathrm{cells\,mL}^{-1}$ and $C(0) = 5\ \mu\mathrm{g\,mL}^{-1}$, as well as $r_a = 0.2946\ \mathrm{h}^{-1}$ and $K_a = 3.1507 \times 10^7\ \mathrm{cells\,mL}^{-1}$. As described in chapter 2, we assume an exponential decay and a zero supply rate for beta-lactam by setting $\lambda = 0.2589\ \mathrm{h}^{-1}$ and $\theta = 0\ \mu\mathrm{g\,mL}^{-1}\,\mathrm{h}^{-1}$ as before. Additionally for this new model, we fix $\gamma = 0.05\ \mathrm{h}^{-1}$, which is a plausible value for the degradation of signal molecules [13]. Hence, we obtain the parameter values in table 3.3.

Parameter	Meaning	Value	Unit
r_a	Intrinsic growth rate of type A	0.2946^*	h^{-1}
K_a	Carrying capacity of type A	$3.1507 \times 10^{7*}$	$\mathrm{cells\,mL}^{-1}$
ε_β	Death rate of type A due to beta-lactam	0.0227	$\mathrm{mL\,h}^{-1}\,\mu\mathrm{g}^{-1}$
ω_1	Mass action coefficient for change from type A into type T	0.3649	$\mathrm{mL\,h}^{-1}\,\mu\mathrm{g}^{-1}$
ω_2	Mass action coefficient for change from type T into type B	0.3798	h^{-1}
δ_n	Natural death rate of type B	0.0018	h^{-1}
θ	Supply rate of beta-lactam	0^*	$\mu\mathrm{g\,mL}^{-1}\,\mathrm{h}^{-1}$
λ	Degradation rate of beta-lactam	0.2589^*	h^{-1}
μ	Signal production coefficient	4.7947×10^{-7}	$\mathrm{mL\,cells}^{-1}\,\mathrm{h}^{-1}$
ν	Maximum rate of production of signal molecules due to autoinduction	1.0985	$\mathrm{mL\,cells}^{-1}\,\mathrm{h}^{-1}$

Parameter	Meaning	Value	Unit
K	Half saturation constant for autoinduction	77.0126	$\mu g\,mL^{-1}$
γ	Degradation rate of signal molecules	0.05^*	h^{-1}
$A(0)$	Initial value of type A	216.8226	$cells\,mL^{-1}$
$T(0)$	Initial value of type T	0^*	$cells\,mL^{-1}$
$B(0)$	Initial value of type B	0^*	$cells\,mL^{-1}$
$C(0)$	Initial value of beta-lactam	5^*	$\mu g\,mL^{-1}$
$S(0)$	Initial value of signal molecules	3.9566×10^{-6}	$\mu g\,mL^{-1}$

Table 3.3: Estimated parameter values of the QS Model, cf. [7]. Values that were fixed before the optimisation procedure are indicated by stars.

The model dynamics and the comparison to the given data for the results in table 3.3 are depicted in figure 3.2.
The congruence of observed and fitted data at the time points 0h, 1h, and 24h is quite exact. However, the model fails to capture the small proportion of rod shaped cells after 4h. When comparing the dynamics to the Naive Model, it seems that there the slopes for the different morphotypes are less steep. In this model we see a small time interval at the beginning where the cell density of rod shaped cells increases slightly before decreasing rapidly. It might be questionable if these more extreme trends are more realistic. The faster decay of the total bacterial density is also remarkable. In the former model there is hardly any decrease noticeable, whereas here it is. Hence one suspects that the system of the QS Model also tends to the trivial equilibrium where no bacteria are left.

Uncertainty of Estimates

Again we investigate the quality and reliability of the estimates and visualise their uncertainty by presenting some heatmaps. The evaluation of the objective function for varying mass action parameters ω_1 and ω_2 is plotted in figure 3.3. Apparently the least squares function shows a local minimum for the fitted values.
The contour plot of the function for different values of ε_β and δ_n in figure 3.4 becomes somewhat more irregular. For a broader range of parameter values two local minima are recognisable. One appears for very small values of ε_β and δ_n, while the other one is located in a region for larger parameter values. By zooming in we can guess that the minimum is smaller for the smaller values of ε_β and δ_n. This can be confirmed by performing two different optimisations. One optimisation is constrained to very small parameter values and the other to the area where the second minimum is attained. The function value for minimisers $\varepsilon_\beta = 0.0227$ and $\delta_n = 0.0018$ equals 0.0014, whereas the second minimum takes the value 0.0462 for minimisers $\varepsilon_\beta = 3.5544$ and $\delta_n = 0.2292$. This confirms the choice of the parameter values.
For parameters μ and ν very fine contour lines are necessary to visualise the minimum of the objective function. Apparently the estimated values minimise the function, however there exists a drawn-out area in figure 3.5. Hence, in this case the minimisers might not be as accurate as others. For reduced tolerances of the solver, the value for μ gets very close to zero.

3.3 Mathematical Analysis

The system of equations (3.1) to (3.5) is more complex than the system of the Naive Model due to the additional equation for the signal molecules. Therefore, we use another approach to determine stationary points. We non-dimensionalise the system and by that reduce the number of parameters which simplifies the analysis. The non-dimensionalisation produces two smoothly orbitally equivalent systems, cf. [21, Chapter 2.1], meaning that we can examine the properties of the non-dimensionalised system instead of the original one since the characteristics are preserved.

We non-dimensionalise the variables in the following way. The time variable t is measured in hours whereas the parameter r_a is measured per hour; hence we can define a dimensionless variable by

$$\tau(t) \coloneqq r_a t.$$

As stated in [28, p. 2], the intrinsic growth rate r_a gives a measure of the dynamics of the population growth and the above transformation explains that $1/r_a$ "is a representative time scale of the response of the model to any change in the population". We analogously non-dimensionalise the other variables:

$$\begin{aligned}
&\tilde{A}(t) \coloneqq K_a^{-1} A(t), \quad \tilde{T}(t) \coloneqq K_a^{-1} T(t), \quad \tilde{B}(t) \coloneqq K_a^{-1} B(t),\\
&\tilde{C}(t) \coloneqq \theta^{-1}\lambda C(t), \quad \tilde{S}(t) \coloneqq K^{-1} S(t).
\end{aligned}$$

Note that these transformations are only possible for strictly positive parameter values of K_a, K, and θ. The case $\theta = 0$ has to be considered separately. For now this leads to the new system

$$\begin{aligned}
\frac{d\tilde{A}}{d\tau}(\tau) &= \tilde{A}(\tau)\left(1 - \tilde{A}(\tau)\right) - \frac{\varepsilon_\beta \theta}{r_a \lambda}\tilde{A}(\tau)\tilde{C}(\tau) - \frac{\omega_1 K}{r_a}\tilde{A}(\tau)\tilde{S}(\tau)\\
\frac{d\tilde{T}}{d\tau}(\tau) &= \frac{\omega_1 K}{r_a}\tilde{A}(\tau)\tilde{S}(\tau) - \frac{\omega_2}{r_a}\tilde{T}(\tau)\\
\frac{d\tilde{B}}{d\tau}(\tau) &= \frac{\omega_2}{r_a}\tilde{T}(\tau) - \frac{\delta_n}{r_a}\tilde{B}(\tau)\\
\frac{d\tilde{C}}{d\tau}(\tau) &= \frac{\lambda}{r_a}\left(1 - \tilde{C}(\tau)\right)\\
\frac{d\tilde{S}}{d\tau}(\tau) &= \left(\frac{K_a\theta}{K r_a \lambda}\mu + \frac{\frac{K_a\theta}{K r_a \lambda}\nu \tilde{S}(\tau)}{1 + \tilde{S}(\tau)}\right)\tilde{A}(\tau)\tilde{C}(\tau) - \frac{\gamma}{r_a}\tilde{S}(\tau).
\end{aligned}$$

To improve legibility we define the dimensionless parameters

$$\begin{aligned}
&\tilde{\varepsilon}_\beta \coloneqq \frac{\varepsilon_\beta \theta}{r_a \lambda}, \quad \tilde{\omega}_1 \coloneqq \frac{\omega_1 K}{r_a}, \quad \tilde{\omega}_2 \coloneqq \frac{\omega_2}{r_a}, \quad \tilde{\delta}_n \coloneqq \frac{\delta_n}{r_a},\\
&\tilde{\lambda} \coloneqq \frac{\lambda}{r_a}, \quad \tilde{\mu} \coloneqq \frac{K_a\theta}{K r_a \lambda}\mu, \quad \tilde{\nu} \coloneqq \frac{K_a\theta}{K r_a \lambda}\nu, \quad \tilde{\gamma} \coloneqq \frac{\gamma}{r_a}.
\end{aligned}$$

By these definitions the number of parameters is reduced by one third from twelve to eight and the system simplifies to

$$\frac{d\tilde{A}}{d\tau}(\tau) = \tilde{A}(\tau)\left(1-\tilde{A}(\tau)\right) - \tilde{\varepsilon}_\beta \tilde{A}(\tau)\tilde{C}(\tau) - \tilde{\omega}_1 \tilde{A}(\tau)\tilde{S}(\tau) \tag{3.6}$$

$$\frac{d\tilde{T}}{d\tau}(\tau) = \tilde{\omega}_1 \tilde{A}(\tau)\tilde{S}(\tau) - \tilde{\omega}_2 \tilde{T}(\tau) \tag{3.7}$$

$$\frac{d\tilde{B}}{d\tau}(\tau) = \tilde{\omega}_2 \tilde{T}(\tau) - \tilde{\delta}_n \tilde{B}(\tau) \tag{3.8}$$

$$\frac{d\tilde{C}}{d\tau}(\tau) = \tilde{\lambda}(1-\tilde{C}(\tau)) \tag{3.9}$$

$$\frac{d\tilde{S}}{d\tau}(\tau) = \left(\tilde{\mu} + \frac{\tilde{\nu}\tilde{S}(\tau)}{1+\tilde{S}(\tau)}\right)\tilde{A}(\tau)\tilde{C}(\tau) - \tilde{\gamma}\tilde{S}(\tau). \tag{3.10}$$

Since equation (3.9) can be solved explicitly by

$$\tilde{C}(\tau) = (\tilde{C}(0)-1)e^{-\tilde{\lambda}\tau} + 1,$$

we can even reduce the system to the four equations

$$\begin{aligned}
\frac{d\tilde{A}}{d\tau}(\tau) &= \tilde{A}(\tau)\left(1-\tilde{A}(\tau)\right) - \tilde{\varepsilon}_\beta \tilde{A}(\tau)[(\tilde{C}(0)-1)e^{-\tilde{\lambda}\tau}+1] - \tilde{\omega}_1 \tilde{A}(\tau)\tilde{S}(\tau) \\
\frac{d\tilde{T}}{d\tau}(\tau) &= \tilde{\omega}_1 \tilde{A}(\tau)\tilde{S}(\tau) - \tilde{\omega}_2 \tilde{T}(\tau) \\
\frac{d\tilde{B}}{d\tau}(\tau) &= \tilde{\omega}_2 \tilde{T}(\tau) - \tilde{\delta}_n \tilde{B}(\tau) \\
\frac{d\tilde{S}}{d\tau}(\tau) &= \left(\tilde{\mu} + \frac{\tilde{\nu}\tilde{S}(\tau)}{1+\tilde{S}(\tau)}\right)\tilde{A}(\tau)[(\tilde{C}(0)-1)e^{-\tilde{\lambda}\tau}+1] - \tilde{\gamma}\tilde{S}(\tau).
\end{aligned}$$

However, we will determine the stationary points of equations (3.6) to (3.10).

Stationary Points of the Non-Dimensionalised System

We need to find values $\tilde{A}^*$, $\tilde{T}^*$, $\tilde{B}^*$, $\tilde{C}^*$, and $\tilde{S}^*$, for which all derivatives of the variables are zero. Equation (3.9) immediately implies that $\tilde{C}^* = 1$. Inserting this into equation (3.6) we obtain

$$\tilde{A}^*(1-\tilde{A}^*-\tilde{\varepsilon}_\beta - \tilde{\omega}_1\tilde{S}^*) = 0, \tag{3.11}$$

and the values $\tilde{T}^*$ and $\tilde{B}^*$ depend on $\tilde{A}^*$ and $\tilde{S}^*$ in the following way:

$$\tilde{T}^* = \frac{\tilde{\omega}_1}{\tilde{\omega}_2}\tilde{A}^*\tilde{S}^* \quad \text{and} \quad \tilde{B}^* = \frac{\tilde{\omega}_1}{\tilde{\delta}_n}\tilde{A}^*\tilde{S}^*.$$

We distinguish between the following two cases in equation (3.11):

- $\tilde{A}^* = 0$: this implies $\tilde{S}^* = 0$, $\tilde{T}^* = 0$, and $\tilde{B}^* = 0$. Thus, the first and trivial stationary point is

$$P_0 := (\tilde{A}_0^*, \tilde{T}_0^*, \tilde{B}_0^*, \tilde{C}_0^*, \tilde{S}_0^*) = (0,0,0,1,0).$$

- $\tilde{A}^* = 1 - \tilde{\varepsilon}_\beta - \tilde{\omega}_1 \tilde{S}^*$: by inserting this into equation (3.10) we get

$$-(\tilde{\omega}_1(\tilde{\mu}+\tilde{\nu})+\tilde{\gamma})\tilde{S}^{*2} + ((\tilde{\mu}+\tilde{\nu})(1-\tilde{\varepsilon}_\beta) - \tilde{\mu}\tilde{\omega}_1 - \tilde{\gamma})\tilde{S}^* + \tilde{\mu}(1-\tilde{\varepsilon}_\beta) = 0.$$

This equation is fulfilled for

$$\tilde{S}_1^* = -\frac{b+W}{N} \quad \text{and} \quad \tilde{S}_2^* = -\frac{b-W}{N},$$

where

$$\begin{aligned} b &\coloneqq \tilde{\gamma} + \tilde{\mu}\tilde{\omega}_1 + (\tilde{\mu}+\tilde{\nu})(\tilde{\varepsilon}_\beta - 1), \\ W &\coloneqq \sqrt{b^2 - 4\tilde{\mu}(\tilde{\gamma} + \tilde{\omega}_1(\tilde{\mu}+\tilde{\nu}))(\tilde{\varepsilon}_\beta - 1)}, \\ N &\coloneqq 2\tilde{\gamma} + 2\tilde{\omega}_1(\tilde{\mu}+\tilde{\nu}). \end{aligned}$$

Hence, there are two additional stationary points

$$\begin{aligned} P_1 &\coloneqq (\tilde{A}_1^*, \tilde{T}_1^*, \tilde{B}_1^*, \tilde{C}_1^*, \tilde{S}_1^*) = \left(\tilde{A}_1^*, \frac{\tilde{\omega}_1}{\tilde{\omega}_2}\tilde{A}_1^*\tilde{S}_1^*, \frac{\tilde{\omega}_1}{\tilde{\delta}_n}\tilde{A}_1^*\tilde{S}_1^*, 1, \tilde{S}_1^*\right) \\ P_2 &\coloneqq (\tilde{A}_2^*, \tilde{T}_2^*, \tilde{B}_2^*, \tilde{C}_2^*, \tilde{S}_2^*) = \left(\tilde{A}_2^*, \frac{\tilde{\omega}_1}{\tilde{\omega}_2}\tilde{A}_2^*\tilde{S}_2^*, \frac{\tilde{\omega}_1}{\tilde{\delta}_n}\tilde{A}_2^*\tilde{S}_2^*, 1, \tilde{S}_2^*\right). \end{aligned}$$

We need to investigate the biological relevance of these points, since the population densities have to be non-negative. Clearly P_0 is biologically meaningful and represents the case of extinction of *P. aeruginosa*. For P_1 and P_2 the analysis becomes more complicated. We distinguish two cases.

- Assume $\tilde{\varepsilon}_\beta > 1$: here we see that $\tilde{A}^* = 1 - \tilde{\varepsilon}_\beta - \tilde{\omega}_1\tilde{S}^* < 0$ for $\omega_1 \geq 0$ and non-negative $\tilde{S}^*$. Hence the non-trivial stationary points are not meaningful in this case.

- Assume $\tilde{\varepsilon}_\beta \leq 1$: then it holds for the square root

$$W = \sqrt{b^2 - 4\tilde{\mu}(\tilde{\gamma} + \tilde{\omega}_1(\tilde{\mu}+\tilde{\nu}))(\tilde{\varepsilon}_\beta - 1)} \geq b.$$

Note that the denominator $N = 2\tilde{\gamma} + 2\tilde{\omega}_1(\tilde{\mu}+\tilde{\nu}) \geq 0$. Thus it follows for $N \neq 0$

$$\tilde{S}_1^* = -\frac{b+W}{N} \leq 0 \quad \text{and} \quad \tilde{S}_2^* = -\frac{b-W}{N} \geq 0.$$

Therefore only $\tilde{S}_2^*$ can be meaningful (except for the case that $\tilde{S}_1^* = 0$). Taking into account the desired non-negativity of $\tilde{A}_2^*$ we obtain another condition for $\tilde{S}_2^*$:

$$0 \leq \tilde{A}_2^* = 1 - \tilde{\varepsilon}_\beta - \tilde{\omega}_1\tilde{S}_2^* \quad \Leftrightarrow \quad \tilde{S}_2^* \leq \frac{1-\tilde{\varepsilon}_\beta}{\tilde{\omega}_1}.$$

Non-negative $\tilde{S}^*$ and $\tilde{A}^*$ imply non-negative $\tilde{T}^*$ and $\tilde{B}^*$ for non-negative parameter values. Hence P_2 is a biologically relevant stationary point under the conditions

$$\tilde{\varepsilon}_\beta \leq 1 \quad \text{and} \quad \tilde{S}_2^* \leq \frac{1-\tilde{\varepsilon}_\beta}{\tilde{\omega}_1}. \tag{3.12}$$

All in all, P_0 and P_2 are the two possible biologically meaningful stationary points, whereas for P_2 the inequalities (3.12) need to be satisfied.

As mentioned above, we need a different consideration for the case $\theta = 0$ where equation (3.4) reduces to

$$\frac{dC}{dt} = -\lambda C(t).$$

The adjusted system of ODEs can be non-dimensionalised analogously as in the previous situation by setting $\tilde{C}(t) := K^{-1}C(t)$ and by defining the dimensionless parameters correspondingly. For the determination of stationary points we can alternatively simply investigate the original system of equations (3.1) to (3.5). It immediately follows that $C^* = 0$. Inserting this into the other equations we obtain $S^* = 0$, $T^* = 0$, $B^* = 0$, and $A^* = 0$ or $A^* = K_a$. Hence, the two stationary points are

$$Q_0 := (0, 0, 0, 0, 0) \quad \text{and} \quad Q_1 := (K_a, 0, 0, 0, 0).$$

This means that in absence of any supply rate for beta-lactam the antibiotics in the system obviously disappear and the bacterial population either goes extinct or the rod shaped cells reach their carrying capacity.

Stability

In the case of a strictly positive θ the general Jacobian matrix of the non-dimensionalised system (3.6) to (3.10) at a point $P = (\tilde{A}(\tau), \tilde{T}(\tau), \tilde{B}(\tau), \tilde{C}(\tau), \tilde{S}(\tau))$ is given by

$$J(P) = \begin{pmatrix} 1 - 2\tilde{A}(\tau) - \tilde{\varepsilon}_\beta \tilde{C}(\tau) - \tilde{\omega}_1 \tilde{S}(\tau) & 0 & 0 & -\tilde{\varepsilon}_\beta \tilde{A}(\tau) & -\tilde{\omega}_1 \tilde{A}(\tau) \\ \tilde{\omega}_1 \tilde{S}(\tau) & -\tilde{\omega}_2 & 0 & 0 & \tilde{\omega}_1 \tilde{A}(\tau) \\ 0 & \tilde{\omega}_2 & -\tilde{\delta}_n & 0 & 0 \\ 0 & 0 & 0 & -\tilde{\lambda} & 0 \\ \alpha \tilde{C}(\tau) & 0 & 0 & \alpha \tilde{A}(\tau) & \frac{\tilde{\nu}\tilde{A}(\tau)\tilde{C}(\tau)}{(1+\tilde{S}(\tau))^2} - \tilde{\gamma} \end{pmatrix}$$

with

$$\alpha = \tilde{\mu} + \frac{\tilde{\nu}\tilde{S}(\tau)}{1 + \tilde{S}(\tau)}.$$

It does not make sense to calculate the eigenvalues of this general matrix since they become too complex. It is self-evident that the signs of the eigenvalues and hence the stability depend on the parameter values.
For the second case where $\theta = 0$, we state the Jacobian matrix of equations (3.1) to (3.5) at a point $Q = (A(t), T(t), B(t), C(t), S(t))$:

$$J(Q) = \begin{pmatrix} r_a - 2\frac{r_a}{K_a} A(t) - \varepsilon_\beta C(t) - \omega_1 S(t) & 0 & 0 & -\varepsilon_\beta A(t) & -\omega_1 A(t) \\ \omega_1 S(t) & -\omega_2 & 0 & 0 & \omega_1 A(t) \\ 0 & \omega_2 & -\delta_n & 0 & 0 \\ 0 & 0 & 0 & -\lambda & 0 \\ \alpha_K C(t) & 0 & 0 & \alpha_K A(t) & \frac{\nu K A(t) C(t)}{(K+S(t))^2} - \gamma \end{pmatrix}$$

with

$$\alpha_K = \mu + \frac{\nu S(\tau)}{K + S(\tau)}.$$

Considering the matrix at the point $Q_0 = (0, 0, 0, 0, 0)$ we obtain

$$J(Q_0) = \begin{pmatrix} r_a & 0 & 0 & 0 & 0 \\ 0 & -\omega_2 & 0 & 0 & 0 \\ 0 & \omega_2 & -\delta_n & 0 & 0 \\ 0 & 0 & 0 & -\lambda & 0 \\ 0 & 0 & 0 & 0 & -\gamma \end{pmatrix}.$$

Obviously only the eigenvalues $-\omega_2$, $-\delta_n$, $-\lambda$, and $-\gamma$ are negative, whereas r_a is positive, making Q_0 an unstable stationary point in our case. When inserting the point $Q_1 = (K_a, 0, 0, 0, 0)$, the Jacobian becomes

$$J(Q_1) = \begin{pmatrix} -r_a & 0 & 0 & -\varepsilon_\beta K_a & -\omega_1 K_a \\ 0 & -\omega_2 & 0 & 0 & \omega_1 K_a \\ 0 & \omega_2 & -\delta_n & 0 & 0 \\ 0 & 0 & 0 & -\lambda & 0 \\ 0 & 0 & 0 & \mu K_a & -\gamma \end{pmatrix}.$$

The eigenvalues $-r_a, -\omega_2$, $-\delta_n$, $-\lambda$, and $-\gamma$ are all negative, which implies that Q_1 is stable. Comparing this outcome with the model dynamics in figure 3.2b the instability of Q_0 is rather counter-intuitive. However, when we run the numerical ODE solution of the original model, equations (3.1) to (3.5), for a longer time interval, MATLAB also calculates a solution where the population density $A(t)$ reaches the carrying capacity, see figure 3.6.

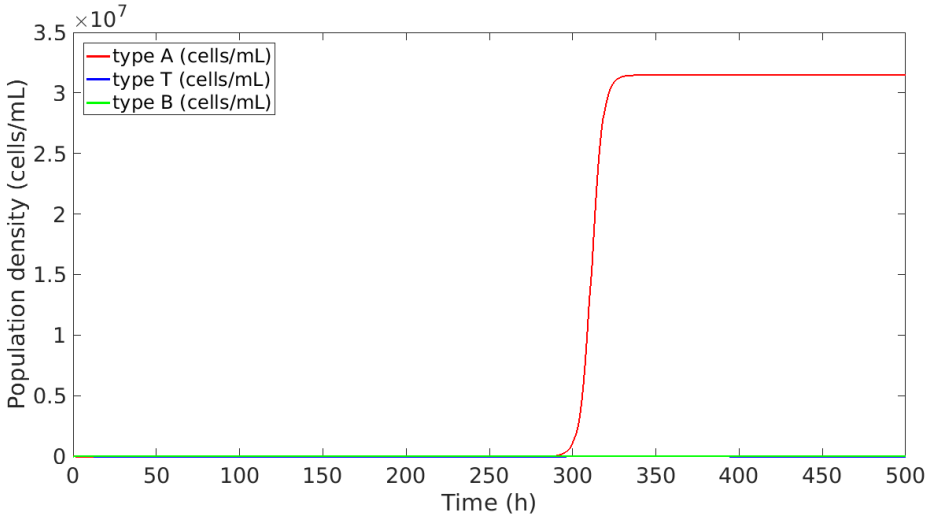

Figure 3.6: Dynamics of the QS Model, equations (3.1) to (3.5), in the long run.

This might suggest that the model is appropriate for the observations in the first days, but in the long run it becomes less meaningful.

Positivity

For checking the positivity of our model, we once more apply proposition 2 and theorem 2. Obviously the right hand side of the dimensionless model (3.6) to (3.10) is Lipschitz-continuous with respect to $(\tilde{A}(\tau), \tilde{T}(\tau), \tilde{B}(\tau), \tilde{C}(\tau), \tilde{S}(\tau))$ and hence there exists a locally unique solution by theorem 2. To use the statement about positivity we need to check that for non-negative variables the derivative of each variable is non-negative if the corresponding variable is set to zero.
Let $(\tilde{A}(\tau), \tilde{T}(\tau), \tilde{B}(\tau), \tilde{C}(\tau), \tilde{S}(\tau))$ be non-negative.

- If $\tilde{A}(\tau) = 0$, then

$$\frac{d\tilde{A}}{d\tau}(\tau) = \tilde{A}(\tau)\left(1 - \tilde{A}(\tau)\right) - \tilde{\varepsilon}_\beta \tilde{A}(\tau)\tilde{C}(\tau) - \tilde{\omega}_1 \tilde{A}(\tau)\tilde{S}(\tau) = 0 \geq 0.$$

- If $\tilde{T}(\tau) = 0$, then

$$\frac{d\tilde{T}}{d\tau}(\tau) = \tilde{\omega}_1 \tilde{A}(\tau)\tilde{S}(\tau) - \tilde{\omega}_2 \tilde{T}(\tau) = \tilde{\omega}_1 \tilde{A}(\tau)\tilde{S}(\tau) \geq 0.$$

- If $\tilde{B}(\tau) = 0$, then

$$\frac{d\tilde{B}}{d\tau}(\tau) = \tilde{\omega}_2 \tilde{T}(\tau) - \tilde{\delta}_n \tilde{B}(\tau) = \tilde{\omega}_2 \tilde{T}(\tau) \geq 0.$$

- If $\tilde{C}(\tau) = 0$, then

$$\frac{d\tilde{C}}{d\tau}(\tau) = \tilde{\lambda}(1 - \tilde{C}(\tau)) = \tilde{\lambda} \geq 0.$$

- If $\tilde{S}(\tau) = 0$, then

$$\frac{d\tilde{S}}{d\tau}(\tau) = \left(\tilde{\mu} + \frac{\tilde{\nu}\tilde{S}(\tau)}{1 + \tilde{S}(\tau)}\right) \tilde{A}(\tau)\tilde{C}(\tau) - \tilde{\gamma}\tilde{S}(\tau) = \tilde{\mu}\tilde{A}(\tau)\tilde{C}(\tau) \geq 0.$$

By that proposition 2 tells us that $\mathbb{R}^4_+$ is a positively invariant domain for the QS Model.

Boundedness

As for the Naive Model we state upper bounds for the five variables. This is done analogously to section 2.3 by transforming the system of equations (3.6) to (3.10) such that we can apply proposition 2.
We claim that the variable $\tilde{A}(\tau)$ is bounded by 1. To show this we transform the original system by introducing the variable $X(\tau) := 1 - \tilde{A}(\tau)$ and replacing $\tilde{A}(\tau)$.

The transformed system is given by

$$\frac{dX}{d\tau}(\tau) = (X(\tau)-1)X(\tau) + \tilde{\varepsilon}_\beta(1-X(\tau))\tilde{C}(\tau) + \tilde{\omega}_1(1-X(\tau))\tilde{S}(\tau) \tag{3.13}$$

$$\frac{d\tilde{T}}{d\tau}(\tau) = \tilde{\omega}_1(1-X(\tau))\tilde{S}(\tau) - \tilde{\omega}_2\tilde{T}(\tau) \tag{3.14}$$

$$\frac{d\tilde{B}}{d\tau}(\tau) = \tilde{\omega}_2\tilde{T}(\tau) - \tilde{\delta}_n\tilde{B}(\tau) \tag{3.15}$$

$$\frac{d\tilde{C}}{d\tau}(\tau) = \tilde{\lambda}(1-\tilde{C}(\tau)) \tag{3.16}$$

$$\frac{d\tilde{S}}{d\tau}(\tau) = \left(\tilde{\mu} + \frac{\tilde{\nu}\tilde{S}(\tau)}{1+\tilde{S}(\tau)}\right)(1-X(\tau))\tilde{C}(\tau) - \tilde{\gamma}\tilde{S}(\tau). \tag{3.17}$$

The solution remains locally unique under this transformation but we need to check the second condition of proposition 2. Therefore we assume that $X(\tau)$, $\tilde{T}(\tau)$, $\tilde{B}(\tau)$, $\tilde{C}(\tau)$, and $\tilde{S}(\tau)$ are non-negative.

- Let $X(\tau) = 0$, then

$$\frac{dX}{d\tau}(\tau) = \tilde{\varepsilon}_\beta\tilde{C}(\tau) + \tilde{\omega}_1\tilde{S}(\tau) \geq 0.$$

- Let $\tilde{T}(\tau) = 0$, then

$$\frac{d\tilde{T}}{d\tau}(\tau) = \tilde{\omega}_1(1-X(\tau))\tilde{S}(\tau) \geq 0,$$

  if $1 - X(\tau) \geq 0$ which is equivalent to $\tilde{A}(\tau) \geq 0$.

- Let $\tilde{B}(\tau) = 0$, then

$$\frac{d\tilde{B}}{d\tau}(\tau) = \tilde{\omega}_2\tilde{T}(\tau) \geq 0.$$

- Let $\tilde{C}(\tau) = 0$, then

$$\frac{d\tilde{C}}{d\tau}(\tau) = \tilde{\lambda} \geq 0.$$

- Let $\tilde{S}(\tau) = 0$, then

$$\frac{d\tilde{S}}{d\tau}(\tau) = \tilde{\mu}(1-X(\tau))\tilde{C}(\tau) \geq 0,$$

  if $1 - X(\tau) \geq 0$.

By proposition 2 it follows under the condition $0 \leq \tilde{A}(0) \leq 1$, that $X(\tau) \geq 0$ which implies that $\tilde{A}(\tau) \leq 1$.
Analogously, we can derive the following bounds for the other variables:

$$\tilde{C}(\tau) \leq 1, \quad \tilde{S}(\tau) \leq \frac{\tilde{\mu}+\tilde{\nu}}{\tilde{\gamma}}, \quad \tilde{T}(\tau) \leq \frac{\tilde{\omega}_1}{\tilde{\omega}_2}\frac{\tilde{\mu}+\tilde{\nu}}{\tilde{\gamma}}, \quad \tilde{B}(\tau) \leq \frac{\tilde{\omega}_1}{\tilde{\delta}_n}\frac{\tilde{\mu}+\tilde{\nu}}{\tilde{\gamma}}.$$

Remark 5 We could also set up a model for the reversion and explain it with QS. However, we rather assume that the cells in their abnormal spherical shape automatically revert in absence of antibiotics and we therefore do not consider an extra model in the case of QS. ◇

3.4 Modifications of the QS Model

In the following we present several modifications of the QS Model (3.1) to (3.5). However, we only give a short intuition for the changes but do not carry out the analytical analyses.

Modification 1

In the QS Model the conversion from type A into type T cells is incorporated by the term $\omega_1 A(t)S(t)$, which is not bounded, i.e. the more signal molecules there are, the more rod cells convert without limitation. Therefore, we introduce the saturation term $\omega_1 A(t)S(t)\,(1 - S(t)/K_S)$. The impact of the signal molecule concentration on conversion becomes less with increasing concentration and if it rises above the maximal value K_S there is no additional effect. By this modification only the first two equations of the dynamical system (3.1) to (3.5) are changed.

$$\frac{dA}{dt} = \underbrace{r_a A(t)\left(1 - \frac{A(t)}{K_a}\right)}_{\text{log. growth}} - \underbrace{\varepsilon_\beta A(t)C(t)}_{\text{death by beta-lactam}} - \underbrace{\omega_1 A(t)S(t)\left(1 - \frac{S(t)}{K_S}\right)}_{\text{conversion to } T} \tag{3.18}$$

$$\frac{dT}{dt} = \underbrace{\omega_1 A(t)S(t)\left(1 - \frac{S(t)}{K_S}\right)}_{\text{conversion to } T} - \underbrace{\omega_2 T(t)}_{\text{conversion to } B} \tag{3.19}$$

$$\frac{dB}{dt} = \underbrace{\omega_2 T(t)}_{\text{conversion to } B} - \underbrace{\delta_n B(t)}_{\text{natural death}} \tag{3.20}$$

$$\frac{dC}{dt} = \underbrace{\theta}_{\text{supply}} - \underbrace{\lambda C(t)}_{\text{degradation}} \tag{3.21}$$

$$\frac{dS}{dt} = \underbrace{\left(\mu + \frac{\nu S(t)}{K + S(t)}\right) A(t)C(t)}_{\text{production with autoinduction}} - \underbrace{\gamma S(t)}_{\text{degradation}} \tag{3.22}$$

To maintain positivity of the system, it is necessary that $S(t) \leq K_S$ since otherwise the derivative of $T(t)$ could become negative if $T(t) = 0$ and $A(t)$, $S(t) \geq 0$ (cf. the second condition in proposition 2). By choosing K_S not smaller than the upper bound for $S(t)$, one can circumvent this issue.
Alternatively one can use a similar term as for autoinduction. The dynamics for rod shaped cells in this case become

$$\frac{dA}{dt} = \underbrace{r_a A(t)\left(1 - \frac{A(t)}{K_a}\right)}_{\text{log. growth}} - \underbrace{\varepsilon_\beta A(t)C(t)}_{\text{death by beta-lactam}} - \underbrace{\omega_1 A(t)\frac{S(t)}{K_S + S(t)}}_{\text{conversion to } T}.$$

The saturation effect of an increasing concentration of signal molecules on the conversion from type A to type T cells also shows up here.

Modification 2

In this modification we change the term for signal molecule production. As mentioned before, signal molecules regulate further functions like biofilm formation or motility, which are not automatically connected to presence of beta-lactam. Hence, it is reasonable to assume a permanent production of signal molecules independent of any antibiotics. We assume that the "background" production is determined through the same production and autoinduction term but only depends on $A(t)$:

$$\frac{dS}{dt} = \underbrace{\left(\mu + \frac{\nu S(t)}{K + S(t)}\right) A(t)C(t)}_{\text{production/autoinduction}} + \underbrace{\left(\mu + \frac{\nu S(t)}{K + S(t)}\right) A(t)}_{\text{permanent production/autoinduction}} - \underbrace{\gamma S(t)}_{\text{degradation}} .$$

The whole system is then given by

$$\frac{dA}{dt} = \underbrace{r_a A(t)\left(1 - \frac{A(t)}{K_a}\right)}_{\text{log. growth}} - \underbrace{\varepsilon_\beta A(t)C(t)}_{\text{death by beta-lactam}} - \underbrace{\omega_1 A(t)S(t)}_{\text{conversion to } T} \tag{3.23}$$

$$\frac{dT}{dt} = \underbrace{\omega_1 A(t)S(t)}_{\text{conversion to } T} - \underbrace{\omega_2 T(t)}_{\text{conversion to } B} \tag{3.24}$$

$$\frac{dB}{dt} = \underbrace{\omega_2 T(t)}_{\text{conversion to } B} - \underbrace{\delta_n B(t)}_{\text{natural death}} \tag{3.25}$$

$$\frac{dC}{dt} = \underbrace{\theta}_{\text{supply}} - \underbrace{\lambda C(t)}_{\text{degradation}} \tag{3.26}$$

$$\frac{dS}{dt} = \underbrace{\left(\mu + \frac{\nu S(t)}{K + S(t)}\right) A(t)(1 + C(t))}_{\text{production with autoinduction}} - \underbrace{\gamma S(t)}_{\text{degradation}} \tag{3.27}$$

Modification 3

We can also combine the two latter modifications, i.e. we combine the bounded conversion with the changed signal molecule production.

$$\frac{dA}{dt} = \underbrace{r_a A(t)\left(1 - \frac{A(t)}{K_a}\right)}_{\text{log. growth}} - \underbrace{\varepsilon_\beta A(t)C(t)}_{\text{death by beta-lactam}} - \underbrace{\omega_1 A(t)S(t)\left(1 - \frac{S(t)}{K_s}\right)}_{\text{conversion to } T} \tag{3.28}$$

$$\frac{dT}{dt} = \underbrace{\omega_1 A(t)S(t)\left(1 - \frac{S(t)}{K_s}\right)}_{\text{conversion to } T} - \underbrace{\omega_2 T(t)}_{\text{conversion to } B} \tag{3.29}$$

$$\frac{dB}{dt} = \underbrace{\omega_2 T(t)}_{\text{conversion to } B} - \underbrace{\delta_n B(t)}_{\text{natural death}} \tag{3.30}$$

$$\frac{dC}{dt} = \underbrace{\theta}_{\text{supply}} - \underbrace{\lambda C(t)}_{\text{degradation}} \tag{3.31}$$

$$\frac{dS}{dt} = \underbrace{\left(\mu + \frac{\nu S(t)}{K + S(t)}\right) A(t)(1 + C(t))}_{\text{production with autoinduction}} - \underbrace{\gamma S(t)}_{\text{degradation}} \tag{3.32}$$

Modification 4

Campos et al. showed in [7] that the effect of autoinduction on the bacterial population can be little. For that reason we introduce a model without autoinduction, where the signal molecule production occurs only at a constant background rate μ. It depends on the concentration of rod shaped cells $A(t)$ and is augmented by beta-lactam.

$$\frac{dA}{dt} = \underbrace{r_a A(t)\left(1 - \frac{A(t)}{K_a}\right)}_{\text{log. growth}} - \underbrace{\varepsilon_\beta A(t)C(t)}_{\text{death by beta-lactam}} - \underbrace{\omega_1 A(t)S(t)}_{\text{conversion to } T} \tag{3.33}$$

$$\frac{dT}{dt} = \underbrace{\omega_1 A(t)S(t)}_{\text{conversion to } T} - \underbrace{\omega_2 T(t)}_{\text{conversion to } B} \tag{3.34}$$

$$\frac{dB}{dt} = \underbrace{\omega_2 T(t)}_{\text{conversion to } B} - \underbrace{\delta_n B(t)}_{\text{natural death}} \tag{3.35}$$

$$\frac{dC}{dt} = \underbrace{\theta}_{\text{supply}} - \underbrace{\lambda C(t)}_{\text{degradation}} \tag{3.36}$$

$$\frac{dS}{dt} = \underbrace{\mu A(t)(1 + C(t))}_{\text{production}} - \underbrace{\gamma S(t)}_{\text{degradation}} \tag{3.37}$$

Modification 5

Following the ideas in [7] further, we completely leave out the dependency on $C(t)$ in the signal molecule production and assume that only $A(t)$ and $S(t)$ induce it. This is actually the original approach for modelling QS [27, 9].

$$\frac{dA}{dt} = \underbrace{r_a A(t)\left(1 - \frac{A(t)}{K_a}\right)}_{\text{log. growth}} - \underbrace{\varepsilon_\beta A(t)C(t)}_{\text{death by beta-lactam}} - \underbrace{\omega_1 A(t)S(t)}_{\text{conversion to } T} \tag{3.38}$$

$$\frac{dT}{dt} = \underbrace{\omega_1 A(t)S(t)}_{\text{conversion to } T} - \underbrace{\omega_2 T(t)}_{\text{conversion to } B} \tag{3.39}$$

$$\frac{dB}{dt} = \underbrace{\omega_2 T(t)}_{\text{conversion to } B} - \underbrace{\delta_n B(t)}_{\text{natural death}} \tag{3.40}$$

$$\frac{dC}{dt} = \underbrace{\theta}_{\text{supply}} - \underbrace{\lambda C(t)}_{\text{degradation}} \tag{3.41}$$

$$\frac{dS}{dt} = \underbrace{\left(\mu + \frac{\nu S(t)}{K + S(t)}\right) A(t)}_{\text{production with autoinduction}} - \underbrace{\gamma S(t)}_{\text{degradation}} \tag{3.42}$$

Modification 6

At last we modify the term for autoinduction by replacing the linear behaviour by a quadratic term:

$$\frac{dA}{dt} = \underbrace{r_a A(t)\left(1 - \frac{A(t)}{K_a}\right)}_{\text{log. growth}} - \underbrace{\varepsilon_\beta A(t)C(t)}_{\text{death by beta-lactam}} - \underbrace{\omega_1 A(t)S(t)}_{\text{conversion to } T} \tag{3.43}$$

$$\frac{dT}{dt} = \underbrace{\omega_1 A(t)S(t)}_{\text{conversion to } T} - \underbrace{\omega_2 T(t)}_{\text{conversion to } B} \tag{3.44}$$

$$\frac{dB}{dt} = \underbrace{\omega_2 T(t)}_{\text{conversion to } B} - \underbrace{\delta_n B(t)}_{\text{natural death}} \tag{3.45}$$

$$\frac{dC}{dt} = \underbrace{\theta}_{\text{supply}} - \underbrace{\lambda C(t)}_{\text{degradation}} \tag{3.46}$$

$$\frac{dS}{dt} = \underbrace{\left(\mu + \frac{\nu S(t)^2}{K^2 + S(t)^2}\right) A(t)(1 + C(t))}_{\text{production with autoinduction}} - \underbrace{\gamma S(t)}_{\text{degradation}} \tag{3.47}$$

In chapter 4 we compare all presented models and modifications of both the naive and the QS approach.

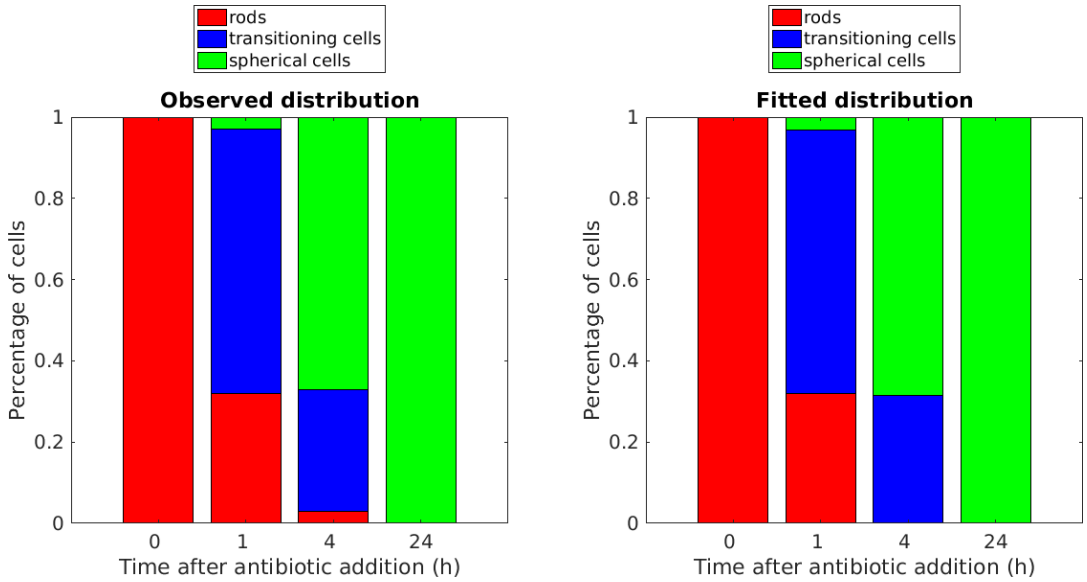

(a) Comparison of the observed (left) and the fitted data (right).

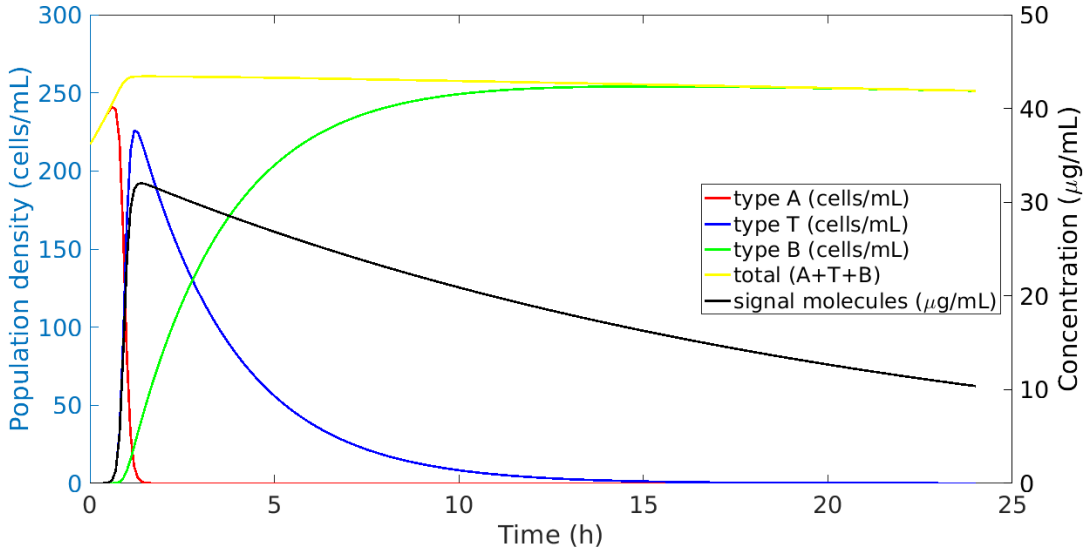

(b) Dynamics of the QS Model for the fitted parameter values.

Figure 3.2: Comparison and dynamics for the fitted parameter values of the QS Model.

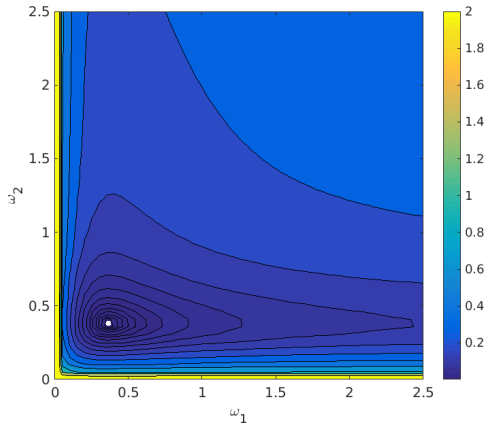

(a) $(\omega_1, \omega_2) \in [0,\ 2.5] \times [0,\ 2.5]$.

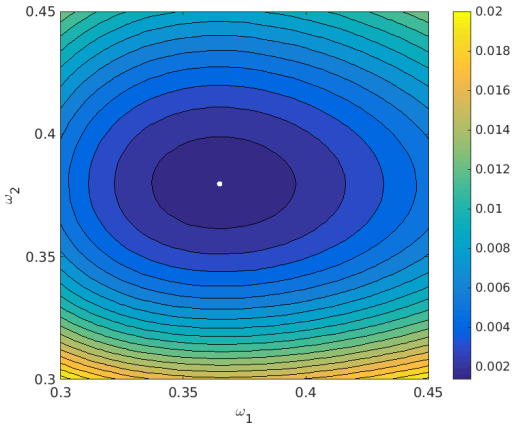

(b) $(\omega_1, \omega_2) \in [0.3,\ 0.45] \times [0.3,\ 0.45]$.

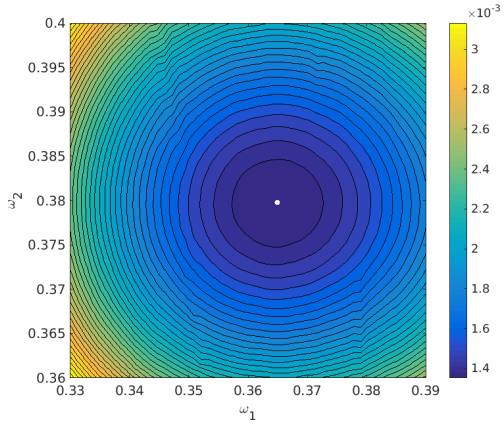

(c) $(\omega_1, \omega_2) \in [0.33,\ 0.39] \times [0.36,\ 0.4]$.

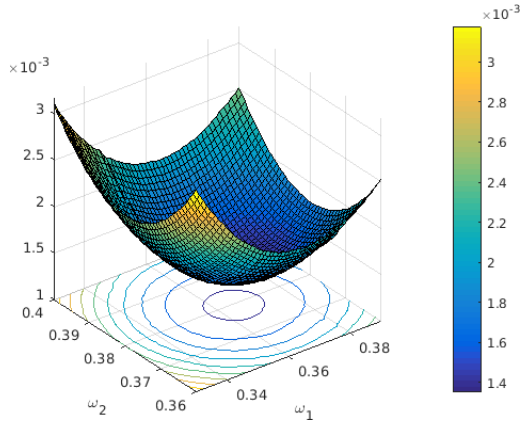

(d) Contour plot of the least squares function depending on ω_1 and ω_2.

Figure 3.3: Evaluation of the least squares function with varying parameters ω_1 and ω_2. Estimated minimum is indicated as white dot.

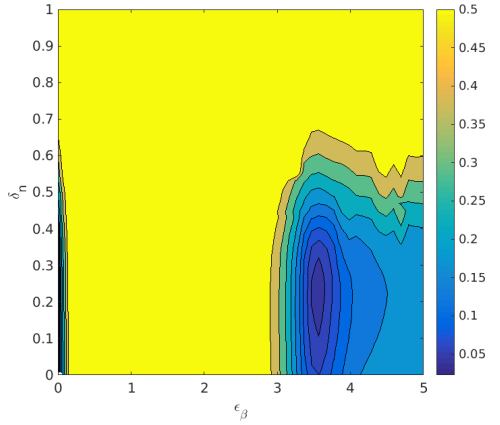

(a) $(\varepsilon_\beta, \delta_n) \in [0,\ 5] \times [0,\ 1]$.

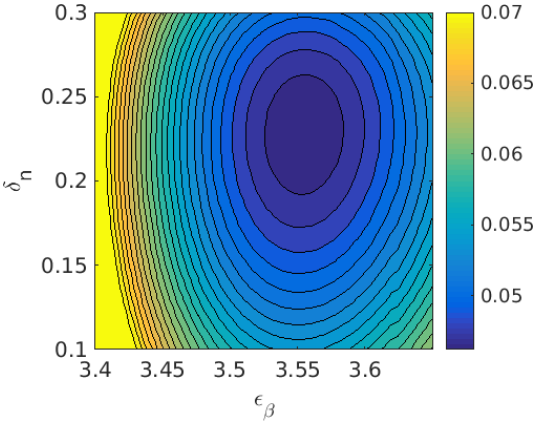

(b) $(\varepsilon_\beta, \delta_n) \in [3.4,\ 3.65] \times [0.1,\ 0.3]$.

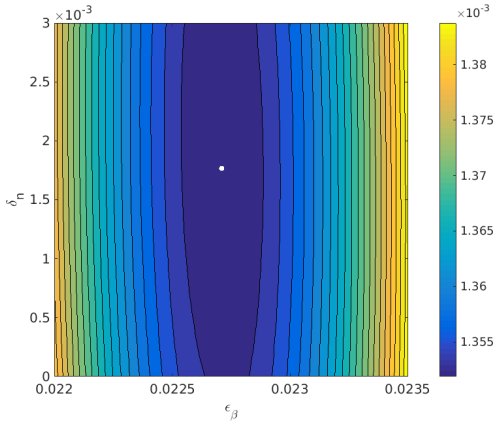

(c) $(\varepsilon_\beta, \delta_n) \in [0.022,\ 0.0235] \times [0,\ 0.003]$.

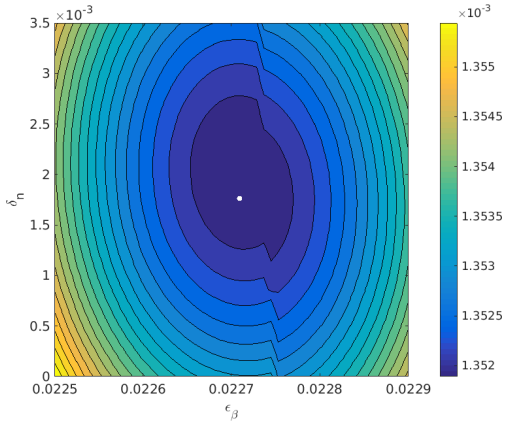

(d) $(\varepsilon_\beta, \delta_n) \in [0.0225,\ 0.0229] \times [0,\ 0.0035]$.

Figure 3.4: Evaluation of the least squares function with varying parameters ε_β and δ_n. Estimated minimum is indicated as white dot.

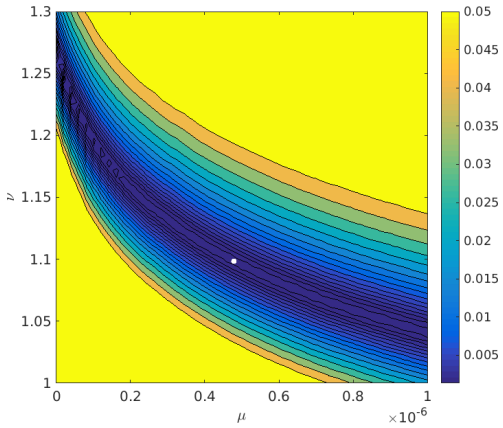

(a) $(\mu, \nu) \in [0,\ 10^{-6}] \times [1,\ 1.3]$.

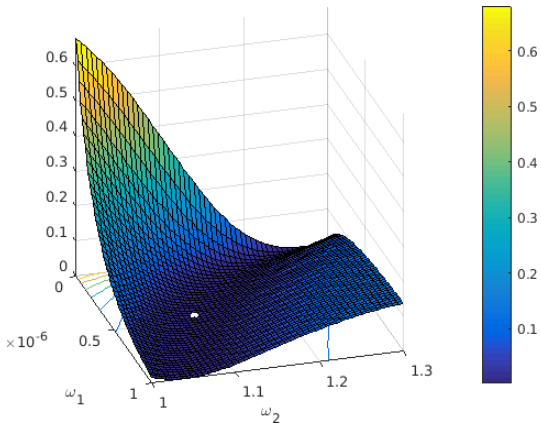

(b) Contour plot of the least squares function depending on μ and ν.

Figure 3.5: Evaluation of the least squares function with varying parameters μ and ν. Estimated minimum is indicated as white dot.

Discussion

4.1 Model Selection

A considerable issue in this thesis is the mismatch of amount of available data and number of parameters in the models. Technically there are insufficient, i.e. too few and poor, data points to use them for parameter fitting. However, we only aimed to develop general models for the biological behaviour. Since we did not know in which range reasonable parameters of the models lie, the data was helpful to obtain a rough idea of the values. We do not want to read too much into the parameter values but rather concentrate on the general behaviour and conclusions from the models.
We still want to compare the models statistically and hence we will use the data nevertheless to determine which model captures the biological observations best. Therefore, we rate the models by a selection criterion, which takes into account both a measure for the goodness of the model's fit to the data and a measure for its complexity. Goodness of fit is measured by the maximum log likelihood $\log(\mathcal{L}(\hat{\theta}|\mathcal{D}))$ of a model, whereas complexity takes into account the number of parameters used in a model [32]. Clearly, complexity should be penalised since otherwise more elaborate models would be preferred, which are not necessarily more explanatory and tend to overfitting. Functionals of these measures are so-called information criteria. The historically oldest one is "a new estimate minimum information theoretical criterion (AIC)" [1] announced by Akaike in 1971 and formally published a few years later [1, 6, 32]. Given a set of models it ranks the adaption of each model to the data relatively to the others by the measure

$$\text{AIC} = 2k - 2\log(\mathcal{L}(\hat{\theta}|\mathcal{D})), \tag{4.1}$$

where the maximum log likelihood $\log(\mathcal{L}(\hat{\theta}|\mathcal{D}))$ is subtracted from the number of estimable parameters k (including σ^2) in the model. According to this criterion, the preferred model is the one with minimum AIC value. There are different formulations of the criterion of which one directly uses the results from least squares estimation. If the models in the collection assume normally distributed errors with a constant variance σ^2, then the AIC can be computed as

$$\text{AIC} = n\log\left(\hat{\sigma}^2\right) + 2k, \tag{4.2}$$

where n is the number of data points, k the number of parameters and

$$\hat{\sigma}^2 = \frac{1}{n}\sum_{i=1}^{4}\sum_{j=1}^{3}(\hat{\mathcal{D}}_{ij} - \mathcal{D}_{ij})^2$$

is the maximum likelihood estimator of σ^2 with estimated residuals

$$\hat{D}_{ij} - D_{ij}, \quad i, j \in \{1, \dots, 4\}.$$

For further reading we refer to [6].
An issue in our situation is the very small sample size $n = 12$ (four time points a three types) compared to the number of estimated parameters k. Therefore, it is recommended to use the so-called AICc, which is a second-order, bias adjusted variant of AIC studied by Sugiura, Hurvich, and Tsai [6]. The measure is given by

$$\text{AICc} = \text{AIC} + \frac{2k(k+1)}{n-k-1}. \tag{4.3}$$

If n is large with respect to k the second term goes to zero and AICc tends to the original AIC. Table 4.1 indicates the corresponding number of parameters k estimated in each model. Note that for linear models k is the total number of estimated parameters, including the intercept and σ^2 [6]. Since our models are non-linear, we do not have an intercept, but we have to include σ^2 even though we do not estimate it explicitly.

Model	**least squares value**	k	**AIC**	**AICc**
Naive Model	0.0184422	6	-65.7362	-0.4894
Modification	0.0182852	6	-65.8388	-0.4904
QS Model	0.0013519	10	-89.0937	1.3091
Modification 1	0.0013639	11	-86.9881	
Modification 2	0.0013546	10	-89.0695	1.3093
Modification 3	0.0013570	11	-87.0489	
Modification 4	0.0091717	8	-70.1184	-0.2212
Modification 5	0.0013525	10	-89.0882	1.3091
Modification 6	0.0013505	10	-89.1065	1.3089

Table 4.1: Least squares value, number of estimated parameters, AIC, and AICc for different models. Computations are shown in listing 8.

Note that one cannot deduce anything from the absolute values of AIC and AICc but only from the relation of these numbers. AIC prefers the QS Models, with Modification 6 showing the best measure. This means that in comparison to the other models the observations are captured best by the model which explains the conversion of rod cells with the help of QS and which contains a non-linear autoinduction term. However, AICc rates the naive approach best, since this criterion penalises the number of parameters much more than AIC. Especially the nutrient dependent growth seems to provide a better balance between number of parameters and fit to the data than the other models. AICc of Modification 1 and 3 is not defined since the number of parameters is eleven leading to a zero denominator in equation (4.3). Nevertheless, the information criteria only compare the models in the set at hand but do not tell how good they actually depict the observations in an absolute sense.
Another criterion is the Bayesian information criterion (BIC) or Schwarz criterion. It is very similar to the AIC but it penalises the number of parameters to a larger extend. It is given by

$$\text{BIC} = \log(n)k - 2\log(\mathcal{L}(\hat{\theta}|\mathcal{D})), \tag{4.4}$$

where k is again the number of parameters, $\log(\mathcal{L}(\hat{\theta}|\mathcal{D}))$ the maximum log likelihood, and n the number of data points. Also for BIC the model with the lowest value is selected. It has been noted that "BIC does well at getting the correct order in large samples, whereas AICc tends to be superior in smaller samples where the relative number of parameters is large" [34]. Hence, in our case it seems reasonable to use the AICc.
Moreover, it should be pointed out that there are studies on more sophisticated model selection for non-linear models. However, the introduced information criteria are widely used also for non-linear models. Since it is not a main aspect of this work, we stick to the common criteria.

4.2 Additional Remarks

The initial values for transitioning and spherical cells are set equal to zero before the optimisation procedure since this is a reasonable value and rather intuitive. The initial concentration of beta-lactam is given in the paper [25]. In contrast, the starting values $A(0)$ of the bacterial population and $S(0)$ of signal molecules are unknown. The paper does not provide any information about the absolute concentration of rods and obviously not about signal molecules. Hence we estimate them together with the other parameters, which possibly allows for a better fit of the parameters than using arbitrarily chosen initial values.
Another issue to point out is that we are given proportions of the different cell types but no absolute values. At every time point these proportions add up to one and hence the proportion of one morphologic type can be computed from the others. This special type of non-negative multivariate data whose sum is constant is called compositional data [41]. In the implementation of the least squares function it is left as an option whether all three cell types should be compared or only two of them, see listing 2. According to some authors compositional data has to be treated in a totally different way than data in absolute numbers. There are different approaches known of how to deal this special data and recent results can be found in [41]. However, it is also common to handle compositional data without any special treatments, as we did here. Since we obtain reasonable results there is no real need for more demanding methods.
As mentioned in the introduction to the concept of QS, the concentration of signal molecules depends on changes in the bacterial cell density and presumably on environmental stress. A certain threshold of the concentration in turn is important for alteration in gene expression. Therefore, it is substantial that the signal molecules are produced quite fast in response to environmental stress because this is essential to induce any change in gene expression. If the whole process would be too slow and the dose of antibiotics high, one rather expects that the critical threshold of signal molecule concentration is not reached fast enough.

4.3 Model Extensions

We present some ideas for further modifications of the introduced models but without any detailed formulation or analysis.
Obviously one can combine the modifications introduced so far. One possibility is to model the growth term in the QS Model also nutrient dependent as in the modification of the Naive Model. A drawback of this approach is the increase of the system to six equations.

In addition, the exponential decay of the beta-lactam can be modified. One can change the fixed zero supply rate to a non-zero value. Alternatively one can simply use another underlying model, different from exponential decay.
Furthermore, one can incorporate the threshold for the signal molecule concentration in the QS system above which gene expression is altered. However, this parameter also has to be estimated by parameter fitting or a plausible value has to be found by literature study. Since the QS approach is only a hypothesis, it suffices to model the presented simplified version as initial attempt.
Moreover, we supposed that only rods - but no transitioning or spherical cells - produce signal molecules. This assumption can be changed by supposing that also cells of other types or different subpopulations of the whole population produce signal molecules.
Additionally one can include a delay in the model: one can assume that cells have to stay in the transitioning state for a while before they convert into spherical cells. However, this complicates the model considerably.
It also might be reasonable to include an extra beta-lactam induced death rate for transitioning cells. From the description of the biological observations we do not know the effect of antibiotics on this cell type.
Finally, we get back to an observation explained at the very beginning but which we did not consider so far: the spherically shaped cells are highly fragile after treatment with beta-lactam and this weakness can be exploited by AMPs, which kill the spherical cells quite efficiently. For setting up a model including AMP treatment, an additional equation similar to the one for beta-lactam is necessary. Furthermore, the equation for spherically shaped cells has to be adjusted by a term that expresses death due to AMPs.

4.4 Conclusion and Outlook

The biological findings by Monahan et al. in [25] were taken up by other researchers. Dörr et al. report in [10, 11] a similar conversion in *Vibrio cholerae* as for *P. aeruginosa*. Under treatment with cell wall synthesis inhibitors, the rod shaped cells transform into viable but non-dividing spherical cells. Viducic et al. studied the tolerance of *P. aeruginosa* to antibiotic stress and how this is associated to the process of QS. They found that RpoN, a protein needed to initiate RNA synthesis, plays an important role in both the regulation of QS and the bacterium's survival strategy in the presence of carbapenems [42]. Their findings support our hypothesis that QS might be relevant for the bacteria's tolerance to beta-lactam antibiotics.

In this thesis we set up different models for the conversion of *P. aeruginosa* from rods to spherical shape under treatment with beta-lactam antibiotics. The Naive Model without any specific biological assumptions about the transition process as well as the QS Model both seem to depict the biological behaviour. We examined and analysed the models with respect to stationary points, stability, and biological relevance, and we were especially interested in whether the observations could be explained by the QS approach. Even though the bacterial population does not go extinct in the long run, the model can match the biological observations. Hence, from a mathematical point of view QS could be linked to the conversion of *P. aeruginosa*.

Parameter Estimation for Different Growth Models

Table A.1 shows growth data of *P. aeruginosa* in a batch culture. The time scale is given in hours and the bacteria are measured in number of cells per micro litre.

Time (h)	**Cells** (μL^{-1})
0	230
3	250
6	350
9	300
12	1420
15	1760
18	2120
21	3680
24	6600
27	8700
30	10500
33	24000
36	27800
39	30800
42	31200
45	31600
48	28000

Table A.1: Growth data of *P. aeruginosa*. Received from Prof. Dr. C. Kuttler (personal communication, 04/04/2017).

We will use this data for our parameter estimation. There are different growth models for *P. aeruginosa*. One example is a nutrient or substrate dependent growth with a corresponding nutrient uptake function, see for example [5, 8]. Another possible model is logistic growth, which we consider first.

A.1 Logistic Growth

We aim to model the population density $A(t)$ of rod shaped bacteria. We use the familiar Verhulst equation with growth rate r_a and carrying capacity K_a:

$$\frac{dA}{dt}(t) = r_a A(t) \left(1 - \frac{A(t)}{K_a}\right).$$

The explicit solution in the case of constant parameters r_a and K_a is well known, see e.g. [26, 28], and is given by

$$A(t) = \frac{A_0 K_a}{e^{-r_a t}(K_a - A_0) + A_0},$$

where A_0 is the initial value of the population.
We estimate the parameters A_0, r_a, and K_a using likelihood estimation (cf. section 2.2). Let $\hat{y}(t_i)$ denote the measured data points in table A.1 at the time points t_i, $i \in \{1, \dots, 17\}$, and let

$$y(t_i, A_0, r_a, K_a) \coloneqq \frac{A_0 K_a}{e^{-r_a t_i}(K_a - A_0) + A_0}$$

represent the "true" values from the model at the corresponding time points. We assume that $\hat{y}(t_i)$ are independent and normally distributed around $y(t_i, A_0, r_a, K_a)$ with some variance $\sigma^2 \geq 0$. The likelihood function is given by

$$\begin{aligned}\mathcal{L}(A_0, r_a, K_a|\hat{y}) &= \prod_{i=1}^{N} P(\hat{y}(t_i) = y(t_i, A_0, r_a, K_a)|A_0, r_a, K_a) \\ &= \prod_{i=1}^{N} \frac{1}{\sqrt{2\pi\sigma^2}} \exp\left(-\frac{(\hat{y}(t_i) - y(t_i, A_0, r_a, K_a))^2}{2\sigma^2}\right),\end{aligned}$$

where $N = 17$ is the number of data points. For computational performances it is better to use the negative log likelihood function

$$\begin{aligned}\mathcal{J}(A_0, r_a, K_a|\hat{y}) &= -\log \mathcal{L}(A_0, r_a, K_a|\hat{y}) \\ &= \frac{N}{2}\log(2\pi\sigma^2) + \sum_{i=1}^{N} \frac{(\hat{y}(t_i) - y(t_i, A_0, r_a, K_a))^2}{2\sigma^2}.\end{aligned}$$

Since we are interested only in the minimisers of this function, it suffices to optimise the least squares function

$$\mathcal{S}(A_0, r_a, K_a|\hat{y}) = \sum_{i=1}^{N} (\hat{y}(t_i) - y(t_i, A_0, r_a, K_a))^2$$

with $y(t_i, A_0, r_a, K_a) = A_0 K_a / (e^{-r_a t_i}(K_a - A_0) + A_0)$.
In order to find the minimum, we perform a multi-start optimisation using 50 randomly sampled parameter values and apply the MATLAB function `fmincon` (cf. section 2.2). We obtain the least squares estimators

$$\begin{pmatrix} A_0 \\ r_a \\ K_a \end{pmatrix} = \begin{pmatrix} 4.2329 \\ 0.2946 \\ 31507 \end{pmatrix},$$

in which A_0 and K_a are measured in $\mathrm{cells}\,\mu\mathrm{L}^{-1}$ and r_a in h^{-1}. The fitted curve in figure A.1 shows the result.

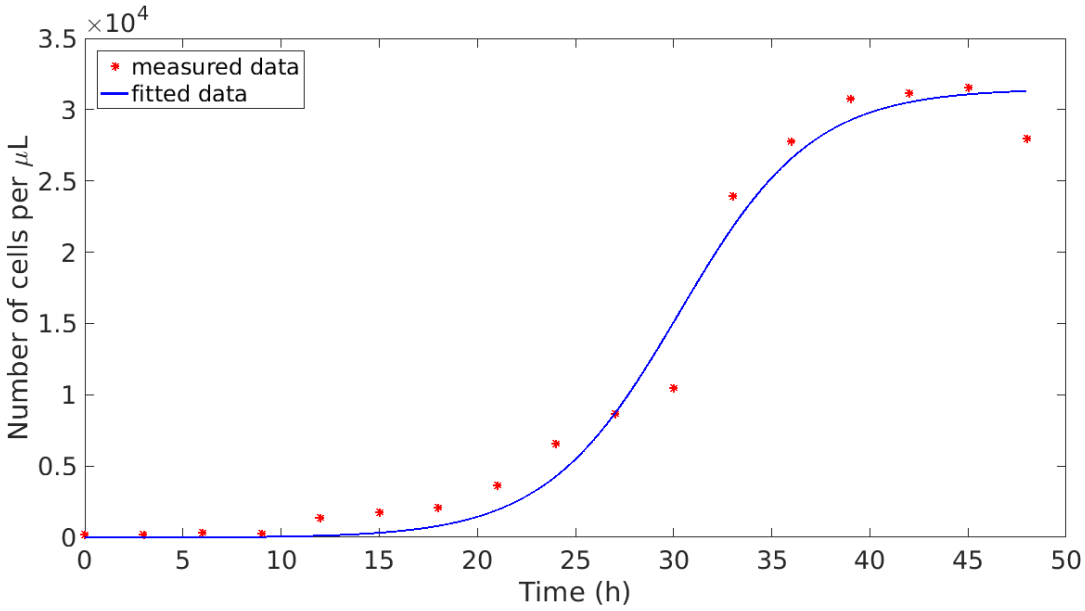

Figure A.1: Parameter estimation for logistic growth of *P. aeruginosa*.

A.2 Nutrient Dependent Growth

As mentioned before, alternatively to the logistic model one can also include a dependency on available nutrients in the system and use a nutrient uptake function. Besides the population density $A(t)$ of rod shaped bacteria we consider the variable $N(t)$ for the concentration of nutrients in the system at time t. Following [5], the dynamics of the nutrients $N(t)$ are expressed by

$$\frac{dN}{dt}(t) = DN(0) - \psi A(t)\frac{N(t)^n}{K_N^n + N(t)^n}, \tag{A.1}$$

where D denotes the inflow of nutrients, ψ the nutrient consumption rate, K_N the nutrient concentration at which half maximum consumption rate is reached, and n expresses non-linearity in the process. The dynamics of the bacterial population can be described by

$$\frac{dA}{dt}(t) = R_a A(t)\frac{N(t)^n}{K_N^n + N(t)^n} \tag{A.2}$$

with growth rate R_a. Note that in equation (A.1) we neglect any abiotic degradation of nutrients by other physical or chemical processes. This is justifiable since the degradation has a much smaller effect on the dynamics than the nutrient uptake. There is no explicit solution available and we need to solve the system of equations (A.1) to (A.2) numerically. As described above, we perform a multi-start optimisation with randomly sampled parameter values for R_a, K_N, ψ, and $A(0)$. The remaining parameter values are taken from [5]: $n = 1.3$, $N(0) = 1$ U, and $D = 0.05\,\mathrm{h}^{-1}$. Here, U stands for some unit that does not have to or cannot be specified. The MATLAB function `fmincon` is used to minimise the least squares function of the measured data and the computed data of the ODE system, cf. section 2.2. Table A.2 summarises the parameters together with their (estimated) values and units.

Parameter	Meaning	Value	Unit
$A(0)$	Initial population density of *P. aeruginosa* of type A (natural rod shape)	92.9731	$\text{cells}\,\mu\text{L}^{-1}$
$N(0)$	Initial concentration of nutrients	$N_0 = 1^*$	U
R_a	Growth rate of type A	0.1663	h^{-1}
K_N	Half saturation constant for consumption	0.0022	U
n	Non-linearity in consumption process	1.3^*	dimensionless
D	Inflow of nutrients	0.05^*	h^{-1}
ψ	Nutrient consumption rate	1.7374×10^{-5}	$\text{U}\,\mu\text{L}\,\text{cells}^{-1}\,\text{h}^{-1}$

Table A.2: Parameter values for the nutrient dependent growth, cf. [5]. Values that were fixed before the optimisation procedure are indicated by stars.

The resulting fit is visualised in figure A.2.

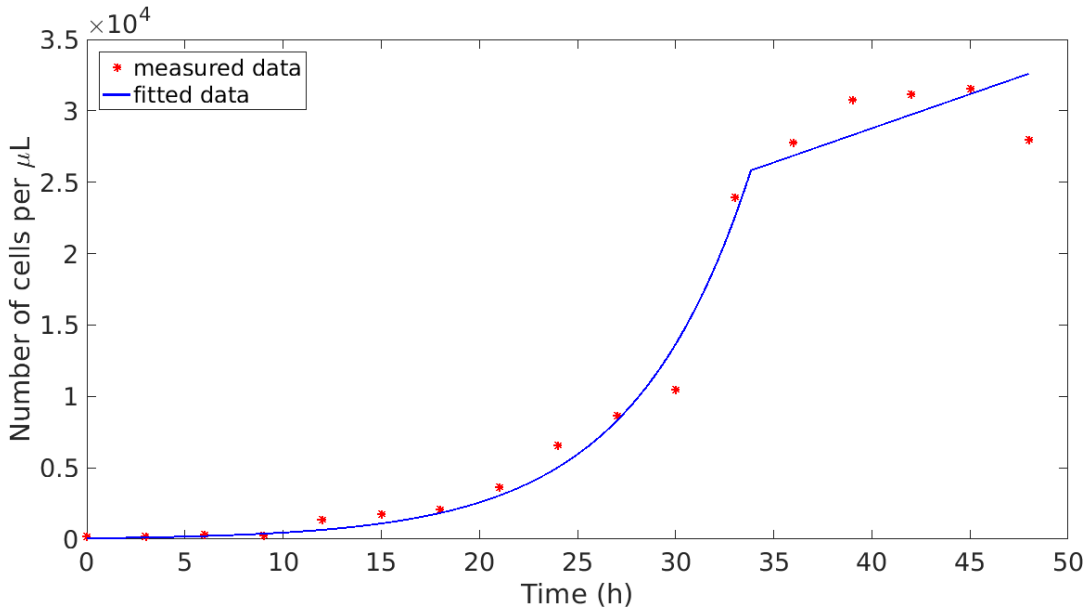

Figure A.2: Parameter estimation for nutrient dependent growth of *P. aeruginosa*.

The shape of the curve at time point 34h stands out because it looks like a kink. But when zooming in, one can see that the course is actually smooth. The ODE solver might have a bad computational performance. However, other solvers give similar results. Nevertheless we use the estimated parameter values since the overall fit looks acceptable.

MATLAB Codes

B.1 Numerical Model Evaluations

In general, the computational analyses and calculations are performed in the same way for the different models. Therefore we only show the codes for the Naive Model but make annotations in case the implementations differ.

Parameter Estimation

For solving the ODE system of the Naive Model, equations (2.1) to (2.4) are encoded in listing 1. The function `odesystem_model1` uses as input the different parameters of the system, including the initial point `y0`, and the time interval `tspan` on which a solution is required. The function returns the numerical solution `sol` of the ODE system together with the corresponding time points in a vector `t`. The different variables $A(t)$, $B(t)$, $T(t)$, and $C(t)$ are redefined as `y(1)`, `y(2)`, `y(3)`, and `y(4)`. The default solver for ODE problems is `ode45`, but there are many more possibilities: stiff ODEs for instance should be solved by special solvers such as `ode15s`. According to [33], non-stiff ODEs can be solved by any solver but to the costs of longer computing times of stiff solvers. Since our problems are not too difficult in comparison to others, `ode15s` still computes a solution in an acceptable time and we are on the safe side in case of stiff ODEs. Furthermore, we follow the advice given in the documentation by The MathWorks, Inc. that one "can improve reliability and efficiency by supplying the Jacobian matrix or its sparsity pattern" [37] when using a stiff solver. Additionally we constrain the solution to be non-negative by setting the option `'NonNegative'` in `opts` to true. Due to bad computational accuracy there appear small negative values if the option is not chosen.

```
1  function [t,sol] = odesystem_model1(r_a, K_a, omega_1, omega_2, e_beta,
     ↪  delta_n, theta, lambda, tspan, y0)
2  % ODE system for the Naive Model
3
4  % define the system of ODEs; y=(A,T,B,C)
5  odefun = @(t,y)[
6    % population density of P. aeruginosa of type A
7    r_a*y(1)*(1-y(1)/K_a) - e_beta*y(1)*y(4) - omega_1*y(1);...
8    % population density of P. aeruginosa of type T
9    omega_1*y(1) - omega_2*y(2);...
10   % population density of P. aeruginosa of type B
11   omega_2*y(2) - delta_n*y(3);...
12   % concentration of beta-lactam C
13   theta - lambda*y(4)];
14
15 % provide the Jacobian
16 J = @(t,y)[
17   r_a*(1-2*y(1)/K_a) - e_beta*y(4) - omega_1, 0, 0, -e_beta*y(1);...
18   omega_1, -omega_2, 0, 0;...
19   0, omega_2, -delta_n, 0;...
```

```
  0, 0, 0, -lambda];

% apply the ODE-solver ode15s
opts = odeset('Stats','off','Jacobian',J,'NonNegative',1);
[t,sol] = ode15s(odefun,tspan,y0,opts);
end
```

Listing 1: ODE system of the Naive Model.

The comparison of the calculated data points with the given data set in form of the least squares value is computed in the function `lsq`. The function uses the input `tspan` - the vector of time points for which the solution `y` of the ODE system is available. Since the cell types are measured in percentages it is possible to disregard one of the types in the comparison and recompute it from the others. The argument `option` indicates which of the cell types, that are written in the three columns of the matrices $\hat{\mathcal{D}}$ and $\mathcal{D}$ respectively, shall be compared. The default is `struct('columns',1:3)`, which means that all types are used for comparison. It is further possible to set `option` equal to `struct('columns',1:2)`, `struct('columns',2:3)`, or `struct('columns',[1,3])`. First the function computes the proportions of the cell types of the calculated solution at the four time points of interest (given by the vector `t`). The result is returned as output `data_new`. The function value of the least squares function is returned as `fval`.

```
function [t,fval,data_new,data] = lsq(tspan, y, option)
% Function for the computation of the least squares value, which has to
 ↪ be minimised.

% check option / set default
if nargin < 3
    option = struct('columns',1:3);
end

% data from bar charts in paper
data = 0.01*[100 0 0; 32 65 3; 3 30 67; 0 0 100];
t = [0 1 4 24];

% construct the matrix with rows for the different time points and
 ↪ columns for different types
A = y(ismember(tspan, t),1:3);
data_new = diag(1./(sum(A,2)))*A;

% least squares value
fval = sum(sum((data(:,option.columns) -
 ↪ data_new(:,option.columns)).^2));
end
```

Listing 2: Least squares function.

For least squares estimation, the latter function `lsq` has to be minimised in order to get the best parameter fit. Fix parameters are stored in the file `variables_fix_model1.mat`, which is loaded at the beginning. For the Naive Model we estimate the mass action parameters ω_1 and ω_2 as well as the parameters ε_β, δ_n and the initial population of rod shaped bacteria $A(0)$. Therefore, we perform a multi-start optimisation using `n` randomly sampled values for every parameter. The MATLAB function `fmincon` starts each optimisation with the sampled points and then calculates a minimum of the objective function. For `fmincon` one can

choose the algorithm that is used to find the minimum, however we stick to the default option `'interior-point'`. Other possibilities are `'active-set'`, `'sqp'`, `'sqp-legacy'`, or `'trust-region-reflective'`. Explanations and details can be found online in the documentation of The MathWorks, Inc. [38]. In order to obtain more accurate results, the option `OptimalityTolerance` is reduced from the default to 10^{-10}.

```
%% Optimisation
clear variables; close all; clc;
cd /home/rebekka/Dokumente/Studium/Masterarbeit/Matlab/model1

% load all parameters and initial values
load('variables_fix_model1.mat');
tspan = 0:0.1:24;
n = 50;

% generate n randomly sampled parameter values
omega_1 = 2*rand(n,1);
omega_2 = 2*rand(n,1);
e_beta = 2*rand(n,1);
delta_n = rand(n,1);
A0 = 200+rand(n,1)*1000;

% predefine matrices and options
MLE = NaN(5,n);             % matrix for MLEs
fval = NaN(1,n);            % vector for function values
options = optimoptions('fmincon', 'Display', 'off', 'Algorithm',
 ↪  'interior-point', 'OptimalityTolerance', 1e-10);

% perform the minimisation for all n starts
tic
fun = @(x) solver(r_a, K_a, x(1), x(2), x(3), x(4), theta, lambda, tspan,
 ↪  [x(5), y0(2:4)]);

for i=1:n
    [MLE(:,i),fval(i),exitflag,output] = fmincon(fun,[omega_1(i),
     ↪  omega_2(i),e_beta(i),delta_n(i),A0(i)],[],[],[],[],[0 0 0 0 0],
     ↪  [5 5 5 5 5000],[],options);
end
toc

% find the minimum of all computations
[fval_sol,j] = min(fval);
% save the fitted parameters of final MLE(:,j)
omega_1 = MLE(1,j);
omega_2 = MLE(2,j);
e_beta = MLE(3,j);
delta_n = MLE(4,j);
A0 = MLE(5,j);

save('variables_MLE_model1.mat','omega_1','omega_2','e_beta','delta_n',
 ↪  'A0','fval_sol');

%% Appendix
function fval = solver(r_a, K_a, omega_1, omega_2, e_beta, delta_n,
 ↪  theta, lambda, tspan, y0)

% calculate ODE solution
[~,y] = odesystem_model1(r_a, K_a, omega_1, omega_2, e_beta, delta_n,
 ↪  theta, lambda, tspan, y0);
% calculate least squares value
```

```
[~,fval,~,~] = lsq(tspan,y);
end
```

Listing 3: Multi-start optimisation of the least squares function.

The model dynamics and the comparison to the given data are visualised by the following code. It uses the fix parameters in `variables_fix_model1.mat` and the newly estimated parameter values in `variables_MLE_model1.mat` for calculating a solution of the ODE system for the fitted parameters. Then the dynamics are plotted over time and a bar chart for the comparison of the given and the calculated data points at the four time points 0, 1, 4, and 24 is created.

```
%% Visualisation
cd /home/rebekka/Dokumente/Studium/Masterarbeit/Matlab/model1

% load fix variables
load('variables_fix_model1.mat');
% load fitted variables
load('variables_MLE_model1.mat');
tspan = 0:0.1:24;

% calculate the ODE solution for the given parameters
tic
[~,y] = odesystem_model1(r_a, K_a, omega_1, omega_2, e_beta, delta_n,
 ↪  theta, lambda, tspan, [A0, y0(2:4)]);
toc

% plot the resulting dynamics
figure
plot(tspan,y(:,1),'r',tspan,y(:,2),'b',tspan,y(:,3),'g',
 ↪  tspan,y(:,1)+y(:,2)+y(:,3),'y','LineWidth',2);
set(gca,'FontSize',20);
xlabel('Time (h)');
ylabel('Population density (cells/mL)');
legend('type A (cells/mL)','type T (cells/mL)','type B (cells/mL)','total
 ↪  (A+T+B)','Location', 'east');

% determine proportions at time points in t, get observed data
[t,~,data_new,data] = lsq(tspan,y);

% plot bar charts
figure
subplot(1,2,1)
Bar1 = bar(data,'stacked');
set(Bar1,{'FaceColor'},{'r';'b';'g'});
set(gca,'FontSize',15);
title('Observed distribution');
xlabel('Time after antibiotic addition (h)');
ylabel('Percentage of cells');
legend('rods','transitioning cells','spherical
 ↪  cells','location','northoutside');
set(gca,'XTickLabel', t);
ylim([0 1]);
subplot(1,2,2)
Bar2 = bar(data_new,'stacked');
set(Bar2,{'FaceColor'},{'r';'b';'g'});
set(gca,'FontSize',15);
title('Fitted distribution');
xlabel('Time after antibiotic addition (h)');
ylabel('Percentage of cells');
legend('rods','transitioning cells','spherical
 ↪  cells','location','northoutside');
```

```
set(gca,'XTickLabel', t);
ylim([0 1]);

save('results_model1.mat','omega_1','omega_2','e_beta',
  ↪  'delta_n','A0','fval_sol','data_new');
```

Listing 4: Visualisation of the Naive Model.

Uncertainty of Estimates

For visualising the uncertainty of the estimates ω_1 and ω_2, we evaluate the least squares function for varying combinations of these two parameters and depict it as heatmap. The different parameter values for ω_1 and ω_2 are generated by the MATLAB function `linspace(a,b,n)`, which returns a row vector of `n` evenly spaced points between `a` and `b` [39]. One example for a filled contour plot and a contour plot under the three-dimensional shaded surface is given below.

```
clear variables; close all; clc;
cd /home/rebekka/Dokumente/Studium/Masterarbeit/Matlab/model1

% load all parameters and initial values
load('variables_fix_model1.mat');
load('variables_MLE_model1.mat');
omega_1_optim = omega_1;
omega_2_optim = omega_2;
tspan = 0:0.1:24;

% vary omega_1 and omega_2
n = 50;
omega_1 = linspace(0.9,1.4,n);
omega_2 = linspace(0.27,0.38,n);
C = NaN(n);

% calculate function values of least squares function
tic
for i=1:n
    for j=1:n
        C(j,i) =
          ↪  solver(r_a,K_a,omega_1(i),omega_2(j),e_beta,delta_n,theta,
          ↪  lambda,tspan,[A0,y0(2:4)]);
    end
end
toc

% plot filled contour plot
figure
contourf(omega_1,omega_2,C,30);
hold on
scatter(omega_1_optim,omega_2_optim,'ow','filled')
set(gca,'FontSize',15);
axis square
xlabel('\omega_1');
ylabel('\omega_2');
colorbar

% plot contour plot under the three-dimensional shaded surface
figure
surfc(omega_1,omega_2,C)
hold on
```

```
scatter(omega_1_optim,omega_2_optim,'ow','filled')
xlabel('\omega_1');
ylabel('\omega_2');
colorbar

%% Appendix
function fval = solver(r_a, K_a, omega_1, omega_2, e_beta, delta_n,
 ↪  theta, lambda, tspan, y0)

% calculate ODE solution
[~,y] = odesystem_model1(r_a, K_a, omega_1, omega_2, e_beta, delta_n,
 ↪  theta, lambda, tspan, y0);
% calculate least squares value
[~,fval,~,~] = lsq(tspan,y);
end
```

Listing 5: Generation of heatmaps for ω_1 and ω_2 in the Naive Model.

Possibly one has to determine the contour levels (last argument of `contourf`) manually as for example in the case of μ and ν by setting

```
v = logspace(-5,log10(0.05),40);
contourf(mu,nu,C,v);
```

The function `logspace(a,b,n)` generates `n` logarithmically spaced points between decades 10^a and 10^b [40].

Model Analysis

To determine stationary points of the system, we solve the right hand side of the model with the help of MATLAB. In principal this can be done nicely using the MATLAB live script, but here we show the standard code for calculating stationary points, the Jacobian, and the eigenvalues of the Jacobian evaluated at the stationary points.

```
% definition of variables and parameters
syms A T B C
syms r_a K_a e_beta omega_1 omega_2 delta_n theta lambda

% definition of RHS of ODE system
ode1 = r_a*A*(1-A/K_a) - e_beta*A*C - omega_1*A;
ode2 = omega_1*A - omega_2*T;
ode3 = omega_2*T - delta_n*B;
ode4 = theta - lambda*C;

% determine equilibria
eqns = [ode1 == 0, ode2 == 0, ode3 == 0, ode4 == 0];
equi = solve(eqns, [A T B C]);
simplify(equi.A)
simplify(equi.T)
simplify(equi.B)
simplify(equi.C)

% determine general Jacobian
odes = [ode1, ode2, ode3, ode4];
J = jacobian(odes, [A T B C])

% J_1
J_1 = simplify(subs(J, [A,T,B,C], [equi.A(1), equi.T(1), equi.B(1),
 ↪  equi.C(1)]))
```

```
eig(J_1)

% J_0
J_0 = subs(J, [A,T,B,C], [equi.A(2), equi.T(2), equi.B(2), equi.C(2)])
eig(J_0)
```

Listing 6: Stationary points of the Naive Model and their stability.

Dependency of the Stationary Point P_1 on ω_1 in the Naive Model

For the Naive Model we want to know where the solution of the ODE system tends to in the long run if we change one of the parameters - in our case ω_1. Therefore, we calculate the ODE solutions for ω_1 varying between zero and $0.5\ \mathrm{h}^{-1}$, extract the population densities after 500 hours, and plot them against ω_1. Additionally, we visualise the population densities of the stationary point P_1 for different values of ω_1.

```
clear variables; close all; clc;
cd /home/rebekka/Dokumente/Studium/Masterarbeit/Matlab/model1

% load fix variables
load('variables_fix_model1.mat');
% load fitted variables
load('variables_MLE_model1.mat');
tspan = 0:0.1:500;
omega_1 = 0:0.01:0.5;
Y=NaN(length(tspan),4,length(omega_1));

% calculate the ODE solution for the given parameters and varying omega_1
for i=1:length(omega_1)
    [~,Y(:,:,i)] = odesystem_model1(r_a, K_a, omega_1(i), omega_2,
     ↪  e_beta, delta_n, theta, lambda, tspan, [A0, y0(2:4)]);
end

% extract the population densities after 500h
Y = squeeze(Y(end,:,:));

% plot the result
figure
plot(omega_1,Y(1,:),'r',omega_1,Y(2,:),'b',omega_1,Y(3,:),'g',
 ↪  'LineWidth',2);
y1=get(gca,'ylim');
hold on
plot([r_a r_a],y1,'--');
set(gca,'FontSize',20);
xlabel('\omega_1 (1/h)');
ylabel('Population density (cells/mL)');
legend('type A (cells/mL)','type T (cells/mL)','type B
 ↪  (cells/mL)','Location', 'northeast');

%% stationary point P1
% calculate the population densities in the stationary point
Sigma = K_a.*(lambda.*r_a-e_beta.*theta-lambda.*omega_1)./(lambda.*r_a);
A1 = Sigma;
T1 = NaN(length(omega_1),1);
B1 = NaN(length(omega_1),1);

for i=1:length(omega_1)
    T1(i) = omega_1(i)./omega_2.*Sigma(i);
    B1(i) = omega_1(i)./delta_n.*Sigma(i);
```

```
41 end
42
43 % plot the population densities in P1
44 figure
45 plot(omega_1,A1,'r',omega_1,T1,'b',omega_1,B1,'g','LineWidth',2);
46 y1=get(gca,'ylim');
47 hold on
48 plot([r_a r_a],y1,'--');
49 set(gca,'FontSize',20);
50 xlabel('\omega_1 (1/h)');
51 ylabel('Population density (cells/mL)');
52 legend('type A (cells/mL)','type T (cells/mL)','type B
    ↪ (cells/mL)','Location', 'southwest');
```

Listing 7: Behaviour of the solution of the Naive Model in the long run for different values of ω_1.

B.2 Model Selection

We show the computation of the information criteria exemplary for the Naive Model. First the function value of the least squares function for the solution is loaded, which then is used in the function `IC(n,k,fval)`. It calculates for the number of data points `n`, the number of fitted parameters `k`, and the function value `fval` the corresponding AIC and AICc.

```
1  n = 12;    % number of sample points
2  % predefine vectors
3  AIC = NaN(10,1);
4  AICc = NaN(10,1);
5  fval = NaN(10,1);
6
7  %% Naive Model (v1):
8  cd /home/rebekka/Dokumente/Studium/Masterarbeit/Matlab/model1
9
10 % load the function value of the solution
11 load('results_model1.mat');
12
13 % determine the AIC/AICc
14 k = 6;
15 [AIC(1), AICc(1)] = IC(n,k,fval_sol);
16 fval(1) = fval_sol;
17
18 %% IC function
19 function [AIC, AICc] = IC(n,k,fval)
20     AIC = 2*k + n*log(fval/n);
21     AICc = AIC + 2*k*(k+1)/(n-k-1);
22 end
```

Listing 8: Computation of AIC and AICc for model selection.

B.3 Growth Models

Logistic Growth

Since we know the explicit solution of the Verhulst equation, we do not need to solve an ODE system. For parameter fitting we only perform a multi-start optimisation of the likelihood function, which equals the least squares function in our case.

```
clear variables; close all; clc;

% given data points
t = 0:3:48;
data = [230, 250, 350, 300, 1420, 1760, 2120, 3680, 6600, 8700, 10500,
 ↪  24000, 27800, 30800, 31200, 31600, 28000];

% generate 50 randomly sampled parameter values
r = 0.5+0.5*rand(50,1);
K = 25000+(35000-25000)*rand(50,1);

MLE = NaN(3,50);              % matrix for MLEs
fval = NaN(1,50);             % vector for function values of the MLEs
options = optimoptions('fmincon', 'Display', 'off');

% optimisation
tic
fun = @(x) lsq_growth(x(1),x(2),x(3),t,data);

for i=1:50
    [MLE(:,i),fval(i)] = fmincon(fun,[data(1),r(i),K(i)],[],[],[],[], [1
     ↪  0.005 20000],[10000 300 50000],[],options);
end
toc

% find the minimum of all computations
[fval_sol,j] = min(fval);
% save the fitted parameters of final MLE(:,j)
A0_sol = MLE(1,j);
r_sol = MLE(2,j);
K_sol = MLE(3,j);

% plot the result
figure
plot(t,data,'*r','LineWidth',2);
hold on
s = 0:0.01:48;
plot(s,(A0_sol.*K_sol) ./
 ↪  (exp(-r_sol.*s).*(K_sol-A0_sol)+A0_sol),'b','LineWidth',2);
set(gca,'FontSize',20);
xlabel('Time (h)');
ylabel('Number of cells per \muL');
legend('measured data','fitted data','Location','northwest');

%% Appendix
function fval = lsq_growth(A0,r,K,t,data)

% calculate the solution
y_true = (A0*K) ./ (exp(-r*t)*(K-A0)+A0);
% calculate least squares value
fval = sum((data-y_true).^2);
end
```

Listing 9: Parameter fitting for the logistic growth model.

Nutrient Dependent Growth

The computations for the nutrient dependent growth run in the same way as the parameter fitting for the models in chapter 2 and chapter 3. We set up a function for

solving the ODE system for the concentration of rod shaped cells $A(t)$ and nutrients $N(t)$.

```
function [t,sol] = odesystem(r_a, K_N, n, D, psi, tspan, y0)
% ODE system for nutrient dependent growth

N0 = y0(2);
% define the system of ODEs; y=(A,N)
odefun = @(t,y)[% growth of P. aeruginosa of type A
              r_a*y(1)*y(2).^n/(K_N.^n+y(2).^n);...
              % concentration of nutrients in the system
              D*N0-psi*y(1)*y(2).^n/(K_N.^n+y(2).^n)];

% apply the ODE-solver ode15s
opts = odeset('Stats','off','NonNegative',1);
[t,sol] = ode15s(odefun,tspan,y0,opts);
end
```

Listing 10: ODE system of the nutrient dependent growth model.

The calculation of the least squares value between the given growth data and the numerical solution is similar as before and we plot the measured points in one plot with the computed solution.

```
clear variables; close all; clc;

% given data points
data = [230, 250, 350, 300, 1420, 1760, 2120, 3680, 6600, 8700, 10500,
 ↪  24000, 27800, 30800, 31200, 31600, 28000];

% define fix parameters
n = 1.3;
N0 = 1;
D = 0.05;
tspan = 0:3:48;
k = 5;

% generate k randomly sampled parameter values
r_a = rand(k,1);
K_N = rand(k,1);
psi = rand(k,1);

MLE = NaN(4,k);             % matrix for MLEs
fval = NaN(1,k);            % vector for function values of the MLEs
options = optimoptions('fmincon', 'Display', 'off');

% perform the minimisation for all k starts
tic
fun = @(x) solver(x(1), x(2), n, D, x(3), tspan, [x(4), N0], data);

for i=1:k
    [MLE(:,i),fval(i)] = fmincon(fun,[r_a(i), K_N(i), psi(i), data(1)],
     ↪  [],[],[],[],[0 0 0 1],[10 100 5 10000],[],options);
end
toc

% find the minimum of all computations
[fval_sol,j] = min(fval)
% save the fitted parameters of final MLE(:,j)
r_a = MLE(1,j);
K_N = MLE(2,j);
```

```
psi = MLE(3,j);
A0 = MLE(4,j);

save('variables_MLE_growth.mat','r_a','K_N','psi','A0','fval_sol');

% calculate ODE solution
[~,y_true] = odesystem(r_a, K_N, n, D, psi, 0:0.01:48, [A0,N0]);

% plot the result
figure
plot(tspan,data,'*r','LineWidth',2);
hold on
plot(0:0.01:48,y_true(:,1),'b','LineWidth',2);
set(gca,'FontSize',20);
xlabel('Time (h)');
ylabel('Number of cells per \muL');
legend('measured data','fitted data','Location','northwest');

%% Appendix
function fval = solver(r_a, K_N, n, D, psi, tspan, y0, data)

% calculate ODE solution
[~,y] = odesystem(r_a, K_N, n, D, psi, tspan, y0);
% extract the data points of type A cells from solution
data_new = y(:,1);
% least squares value
fval = sum((data - data_new').^2);
end
```

Listing 11: Parameter fitting for the nutrient dependent growth model.

[1] H. Akaike. "A New Look at the Statistical Model Identification". In: *IEEE Transactions on Automatic Control* 19.6 (Dec. 1974), pages 716–723. DOI: 10.1109/tac.1974.1100705.

[2] H. Amann. *Gewöhnliche Differntialgleichungen*. 2nd edition. De-Gruyter-Lehrbuch. Berlin, New York: Walter de Gruyter, 1995.

[3] A. Bahar and D. Ren. "Antimicrobial Peptides". In: *Pharmaceuticals* 6.12 (Nov. 2013), pages 1543–1575. DOI: 10.3390/ph6121543.

[4] B. L. Bassler. "How bacteria talk to each other: regulation of gene expression by quorum sensing". In: *Current Opinion in Microbiology* 2.6 (Dec. 1999), pages 582–587. DOI: 10.1016/s1369-5274(99)00025-9.

[5] K. Buddrus-Schiemann et al. "Analysis of N-acylhomoserine lactone dynamics in continuous cultures of *Pseudomonas putida* IsoF by use of ELISA and UHPLC/qTOF-MS-derived measurements and mathematical models". In: *Analytical and Bioanalytical Chemistry* 406.25 (Aug. 2014), pages 6373–6383. DOI: 10.1007/s00216-014-8063-6.

[6] K. P. Burnham and D. R. Anderson. *Model Selection and Multimodel Inference. A Practical Information-Theoretic Approach*. 2nd edition. New York: Springer-Verlag, 2002.

[7] S. Campos et al. *Quorum Sensing Interaction and the Effect of Antibiotic on the Dynamics of Two Strains of the Same Bacterial Species*. Technical Report 2012-13. Mathematics Preprint Series. The University of Texas at Arlington, 2012.

[8] D. L. Chopp et al. "A mathematical model of quorum sensing in a growing bacterial biofilm". In: *Journal of Industrial Microbiology and Biotechnology* 29.6 (Dec. 2002), pages 339–346. DOI: 10.1038/sj.jim.7000316.

[9] J. D. Dockery and J. P. Keener. "A Mathematical Model for Quorum Sensing in *Pseudomonas aeruginosa*". In: *Bulletin of Mathematical Biology* 63.1 (Feb. 2001), pages 95–116. DOI: 10.1006/bulm.2000.0205.

[10] T. Dörr, B. M. Davis and M. K. Waldor. "Endopeptidase-Mediated Beta Lactam Tolerance". In: *PLOS Pathogens* 11.4 (Apr. 2015), e1004850. DOI: DOI:10.1371/journal.ppat.1004850.

[11] T. Dörr et al. "A cell wall damage response mediated by a sensor kinase/response regulator pair enables beta-lactam tolerance". In: *Proceedings of the National Academy of Sciences* 113.2 (Jan. 2016), pages 404–409. DOI: 10.1073/pnas.1520333113.

[12] S. M. Drawz and R. A. Bonomo. "Three Decades of β-Lactamase Inhibitors". In: *Clinical Microbiology Reviews* 23.1 (Jan. 2010), pages 160–201. DOI: 10.1128/CMR.00037-09.

[13] M. Englmann et al. “The hydrolysis of unsubstituted N-acylhomoserine lactones to their homoserine metabolites. Analytical approaches using ultra performance liquid chromatography”. In: *Journal of Chromatography A* 1160.1-2 (Aug. 2007), pages 184–193. DOI: 10.1016/j.chroma.2007.05.059.

[14] R. García-Contreras et al. “Quorum sensing enhancement of the stress response promotes resistance to quorum quenching and prevents social cheating”. In: *The ISME Journal* 9.1 (Jan. 2015), pages 115–125. DOI: doi:10.1038/ismej.2014.98.

[15] M. Z. R. Gomes et al. “Outbreaks, persistence, and high mortality rates of multiresistant *Pseudomonas aeruginosa* infections in a hospital with AIDS-predominant admissions”. In: *The Brazilian Journal of Infectious Diseases* 15.4 (July 2011), pages 312–322. DOI: 10.1016/S1413-8670(11)70198-2.

[16] J. Hasenauer. “Statistical Inference for Stochastic Biochemical Processes”. Lecture notes, Technical University München, WS 2016/2017.

[17] M. Hentzer et al. “Attenuation of *Pseudomonas aeruginosa* virulence by quorum sensing inhibitors”. In: *The EMBO Journal* 22.15 (Aug. 2003), pages 3803–3815. DOI: 10.1093/emboj/cdg366.

[18] A. Izadpanah and R. L. Gallo. “Antimicrobial peptides”. In: *Journal of the American Academy of Dermatology* 52.3 (Mar. 2005), pages 381–390. DOI: 10.1016/j.jaad.2004.08.026.

[19] K.-F. Kong, L. Schneper and K. Mathee. “Beta-lactam Antibiotics: From Antibiosis to Resistance and Bacteriology”. In: *APMIS* 118.1 (Jan. 2010), pages 1–36. DOI: 10.1111/j.1600-0463.2009.02563.x.

[20] C. Kuttler. “Mathematical Models in Biology”. Lecture script, Technical University München, WS 2016/2017.

[21] Y. A. Kuznetsov. *Elements of Applied Bifurcation Theory*. Edited by S. S. Antman, J. E. Marsden and L. Sirovich. 3rd edition. Volume 112. Applied Mathematical Sciences. New York: Springer-Verlag, 2004.

[22] J. Lee and L. Zhang. “The hierarchy quorum sensing network in *Pseudomonas aeruginosa*”. In: *Protein & Cell* 6.1 (Sept. 2014), pages 26–41. DOI: 10.1007/s13238-014-0100-x.

[23] E. Macy. “Penicillin and Beta-Lactam Allergy: Epidemiology and Diagnosis”. In: *Current Allergy and Asthma Reports* 14:476 (Sept. 2014). DOI: 10.1007/s11882-014-0476-y.

[24] M. B. Miller and B. L. Bassler. “Quorum Sensing in Bacteria”. In: *Annual Review of Microbiology* 55.1 (Oct. 2001), pages 165–199. DOI: 10.1146/annurev.micro.55.1.165.

[25] L. G. Monahan et al. “Rapid Conversion of *Pseudomonas aeruginosa* to a Spherical Cell Morphotype Facilitates Tolerance to Carbapenems and Penicillins but Increases Susceptibility to Antimicrobial Peptides”. In: *Antimicrobial Agents and Chemotherapy* 58.4 (Jan. 2014), pages 1956–1962. DOI: 10.1128/aac.01901-13.

[26] J. Müller and C. Kuttler. *Methods and Models in Mathematical Biology. Deterministic and Stochastic Approaches*. Edited by A. Stevens and M. C. Mackey. Lecture Notes on Mathematical Modelling in the Life Sciences. Berlin, Heidelberg: Springer-Verlag, 2015.

[27] J. Müller et al. "Cell-cell communication by quorum sensing and dimension-reduction". In: *Journal of Mathematical Biology* 53.4 (Aug. 2006), pages 672–702. DOI: 10.1007/s00285-006-0024-z.

[28] J. D. Murray. *Mathematical Biology*. Edited by S. A. Levin et al. 2nd edition. Volume 19. Biomathematics. Berlin, Heidelberg: Springer-Verlag, 1993.

[29] D. Nathwani et al. "Clinical and economic consequences of hospital-acquired resistant and multidrug-resistant *Pseudomonas aeruginosa* infections: a systematic review and meta-analysis". In: *Antimicrobial Resistance and Infection Control* 3:32 (Oct. 2014). DOI: 10.1186/2047-2994-3-32.

[30] L. Perko. *Differential Equations and Dynamical Systems*. Edited by F. John et al. Volume 7. Texts in Applied Mathematics. New York: Springer-Verlag, 1991.

[31] K. Poole. "*Pseudomonas aeruginosa:* resistance to the max". In: *Frontiers in Microbiology* 2:65 (Apr. 2011). DOI: 10.3389/fmicb.2011.00065.

[32] H. Rinne. *Taschenbuch der Statistik*. 4th edition. Frankfurt am Main: Verlag Harri Deutsch, 2008.

[33] L. F. Shampine and M. W. Reichelt. "The MATLAB ODE Suite". In: *SIAM Journal on Scientific Computing* 18.1 (Jan. 1997), pages 1–22. DOI: 10.1137/S1064827594276424.

[34] R. H. Shumway and D. S. Stoffer. *Time Series Analysis and Its Applications*. Edited by G. Casella, S. Fienberg and I. Olkin. 3rd edition. Springer Texts in Statistics. New York: Springer, 2011.

[35] H. L. Smith and P. Waltman. *The Theory of the Chemostat. Dynamics of Microbial Competition*. Cambridge University Press, 1995.

[36] R. S. Smith and B. H. Iglewski. "*Pseudomonas aeruginosa* quorum sensing as a potential antimicrobial target". In: *Journal of Clinical Investigation* 112.10 (Nov. 2003), pages 1460–1465. DOI: 10.1172/jci200320364.

[37] The MathWorks, Inc. *Choose an ODE Solver*. 2017. URL: https://de.mathworks.com/help/matlab/math/choose-an-ode-solver.html (visited on 28/06/2017).

[38] The MathWorks, Inc. *fmincon*. 2017. URL: https://de.mathworks.com/help/optim/ug/fmincon.html (visited on 28/06/2017).

[39] The MathWorks, Inc. *linspace*. 2017. URL: https://de.mathworks.com/help/matlab/ref/linspace.html (visited on 07/06/2017).

[40] The MathWorks, Inc. *logspace*. 2017. URL: https://de.mathworks.com/help/matlab/ref/logspace.html (visited on 17/07/2017).

[41] M. Tsagris and C. Stewart. *A Dirichlet Regression Model for Compositional Data with Zeros*. Cornell University Library. 2017. URL: https://arxiv.org/abs/1410.5011v6 (visited on 23/06/2017).

[42] D. Viducic et al. "RpoN Modulates Carbapenem Tolerance in *Pseudomonas aeruginosa* through *Pseudomonas* Quinolone Signal and PqsE". In: *Antimicrobial Agents and Chemotherapy* 60.10 (Oct. 2016), pages 5752–5764. DOI: 10.1128/AAC.00260-16.